



CUY-90-14.90

PID 77332/85531

APPENDIX DR-11

**Internal Energy Dissipator Research for Culverts
(Contract Document)**

State of Ohio
Department of Transportation
Jolene M. Molitoris, Director

**Innerbelt Bridge
Construction Contract Group 1 (CCG1)**

INTERNAL ENERGY DISSIPATORS FOR CULVERTS

by

A.L. Simon and S. Sarikelle

**DEPARTMENT OF CIVIL ENGINEERING
THE UNIVERSITY OF AKRON
AKRON, OHIO 44325**

September 1984

1. Report No. FHWA/OH - 84/007		2. Government Accession No.		3. Recipient's Catalog No.	
4. Title and Subtitle INTERNAL ENERGY DISSIPATORS FOR CULVERTS				5. Report Date SEPTEMBER 1984	
				6. Performing Organization Code	
7. Author(s) A. L. Simon, S. Sarikelle				8. Performing Organization Report No. CEHY84-3	
9. Performing Organization Name and Address Department of Civil Engineering University of Akron Akron, Ohio 44325				10. Work Unit No.	
				11. Contract or Grant No. State Job No. 14350(0)	
12. Sponsoring Agency Name and Address Ohio Department of Transportation P. O. Box 899 Columbus, Ohio 43216				13. Type of Report and Period Covered Final Report	
				14. Sponsoring Agency Code	
15. Supplementary Notes Prepared in cooperation with the U.S. Department of Transportation, Federal Highway Administration.					
16. Abstract Results of a model study of internal energy dissipators for culverts operating under inlet control are given. The study determines the shortest ring chamber design that effectively reduces the outlet velocity. The model results are calibrated with prototype field studies to improve their accuracy. All hydraulic design parameters are discussed and a practical design procedure is given. Ring chamber diameters are found by equations that are functions of the upstream Froude number and flow depth. The lengths before the first dissipator, between each dissipator and after the final dissipator and the size of the dissipators are functions of the ring chamber diameter.					
17. Key Words Culvert, Energy Reduction, Froude Number, Hydraulic Jump, Inlet Control, Internal Energy Dissipator, Model, Prototype, Ring Chamber, Velocity Reduction.			18. Distribution Statement No restrictions. This document is available to the public through the National Technical Information Service, Springfield, Virginia, 22161.		
19. Security Classif. (of this report) Unclassified		20. Security Classif. (of this page) Unclassified		21. No. of Pages	22. Price

Final Report

INTERNAL ENERGY DISSIPATORS FOR CULVERTS

Sponsored by:

Ohio Department of Transportation
and the
U.S. Department of Transportation
Federal Highway Administration

Submitted by:

A. L. Simon and S. Sarikelle
Department of Civil Engineering
The University of Akron
Akron, Ohio 44325

September 1984

DISCLAIMER

The contents of this report reflect the view of the authors who are responsible for the facts and accuracy of the data presented herein. The contents do not necessarily reflect the official views or policies of the Ohio Department of Transportation or the U.S. Department of Transportation Federal Highway Administration. This report does not constitute a standard specification or regulation, nor does mention of trade names or commercial products constitute endorsement for use.

ACKNOWLEDGEMENTS

The authors are indebted to the Ohio Department of Transportation for its continued support for their research of the energy dissipation process in culverts. The success of this study was greatly enhanced by the helpful advice of Messrs. John D. Herl, C. Gene Pettit, and John O. Hurd, all of the Hydraulics Section, Bureau of Location and Design, and Mr. Leon O. Talbert, Engineer of Research and Development, ODOT. The diligent work of Mr. Scott Korom, whose MSCE thesis has partially arisen from this project, is gratefully acknowledged. Mrs. Lynn McCandless' excellent typing of the manuscript is sincerely appreciated.

TABLE OF CONTENTS

	PAGE
LIST OF FIGURES	v
LIST OF TABLES	vii
CHAPTER 1 INTRODUCTION	1
CHAPTER 2 BACKGROUND	2
Section 2.1 The Hydraulic Jump	2
Section 2.2 Development of the Ring Chamber	5
Section 2.3 Hydraulic Modeling for this Study	10
Section 2.4 Froude Numbers for this Study	10
CHAPTER 3 EXPERIMENTAL SETUP	12
Section 3.1 Equipment	12
Section 3.2 Test Procedure	14
CHAPTER 4 RESULTS	17
Section 4.1 Figures 4.1.1 to 4.1.9.	17
Section 4.2 Energy Reduction Graphs	32
Section 4.3 Velocity Reduction Graphs	32
CHAPTER 5 CONCLUSIONS	37
Section 5.1 Hydraulic Design Parameters	37
Section 5.2 Prototype Ring Chamber Tests and Model Calibration	41
Section 5.3 Design Procedure	44
REFERENCES	47
APPENDIX - SAMPLE PROBLEM	49

LIST OF FIGURES

<u>FIGURE</u>		<u>PAGE</u>
2.1.1	THE HYDRAULIC JUMP	4
2.2.1	FULL FLOW RING CHAMBER	6
2.2.2	FREE SURFACE FLOW RING CHAMBER	6
2.2.3.a	OLD 2-PIECE DISSIPATOR	9
2.2.3.b	SECTION C-C	9
2.2.4	4-PIECE DISSIPATOR	9
2.2.5	NEW 2-PIECE DISSIPATOR	9
3.1.1	EXPERIMENTAL SETUP	13
3.2.1	RING CHAMBER FLOWING JUST FULL	15
3.2.2	RING CHAMBER FLOWING FULLY CHOKED	15
4.1.1	PERFORMANCE GRAPH FOR JUST-FULL CONDITIONS; 4 DISSIPATORS; $L/D_o = 1.0$; $K/D_o = 1/8$	22
4.1.2	PERFORMANCE GRAPH FOR FULLY-CHOKED CONDITIONS; 4 DISSIPATORS; $L/D_o = 1.0$; $K/D_o = 1/8$	23
4.1.3	COMPARISON OF FIGURES 4.1.1 AND 4.1.2 AT $D_o/D_i = 1.000$	24
4.1.4	COMPARISON OF FIGURES 4.1.1 AND 4.1.2 AT $D_o/D_i = 1.091$	25
4.1.5	COMPARISON OF FIGURES 4.1.1 AND 4.1.2 AT $D_o/D_i = 1.263$	26
4.1.6	PERFORMANCE GRAPH FOR FULLY-CHOKED CONDITIONS; 3 DISSIPATORS; $L/D_o = 1.0$; $K/D_o = 1/6$	27
4.1.7	COMPARISON OF FIGURES 4.1.2 AND 4.1.6 AT $D_o/D_i = 1.000$	28
4.1.8	COMPARISON OF FIGURES 4.1.2 AND 4.1.6 AT $D_o/D_i = 1.091$	29

LIST OF FIGURES (continued)

<u>FIGURE</u>		<u>PAGE</u>
4.1.9	COMPARISON OF FIGURES 4.1.2 AND 4.1.6 AT $D_0/D_i = 1.263$.	30
4.2.1	BEST-FIT CURVES FOR PERCENT ENERGY REDUCTION	33
4.2.2	BEST-FIT CURVE FOR PERCENT ENERGY REDUCTION	34
4.3.1	BEST-FIT CURVES FOR PERCENT VELOCITY REDUCTION	35
4.3.2	BEST-FIT CURVE FOR PERCENT VELOCITY REDUCTION	36
5.1.1	SUMMARY GRAPH FOR FULLY CHOKED CONDITIONS	38
5.1.2	VENTING REGION	41
5.2.1	CALIBRATED PERCENT VELOCITY REDUCTION CURVE	43

LIST OF TABLES

<u>TABLES</u>		<u>PAGE</u>
4.1.1.a	DATA FOR JUST-FULL CONDITIONS; 4 DISSIPATORS; L/D ₀ = 1.0; K/D ₀ = 1/8	18
4.1.1.b	DATA FOR FULLY-CHOKED CONDITIONS; 4 DISSIPATORS;. L/D ₀ = 1.0; K/D ₀ = 1/8	19
4.1.1.c	DATA FOR FULLY-CHOKED CONDITIONS; 3 DISSIPATORS;. L/D ₀ = 1.0; K/D ₀ = 1/6	20
4.1.2	BEST-FIT EQUATIONS FOR FIGURES 4.1.1, 4.1.2 AND 4.1.6 .	31
5.2.1	COMPARISON OF MODEL AND PROTOTYPE ENERGY REDUCTIONS . .	42
5.3.1	RING CHAMBER DESIGN GUIDE	45

CHAPTER 1

INTRODUCTION

Since the smooth surface of a culvert offers less resistance to flow than a natural stream channel, water usually exits a culvert with a greater velocity than it would if the culvert had not been there. This increase in velocity can lead to excessive erosion or scour downstream and to structural failure of the highway embankment and the culvert itself. For low outlet velocities, lining the downstream channel with rocks offers sufficient protection against erosion and scour. For outlet velocities greater than 18 feet per second, rock protection is not sufficient. These velocities are usually reduced by the formation of a hydraulic jump which pushes the outlet flow to a greater depth and thus produces a lower velocity. The hydraulic jump is usually produced by a rather elaborate energy dissipator constructed at the outlet of the culvert; but if the culvert is on a steep slope and under inlet control, a hydraulic jump can be formed in the culvert itself. This allows the energy dissipator at the culvert exit to be simplified or even eliminated.

A way to form a hydraulic jump in culverts is to place circular rings (roughness elements) on the inside perimeter of the pipe usually near the end section of the pipe. This end section is usually set at a milder slope than the rest of the culvert and is called a ring chamber. The goal of this study was to develop the hydraulic design parameters necessary to design ring chambers that effectively reduce the outlet velocities of culverts on steep slopes and under inlet control by forcing a hydraulic jump to form in the ring chambers.

CHAPTER 2

BACKGROUND

In this chapter the hydraulic jump, the development of ring chambers that form hydraulic jumps, hydraulic modeling and Froude numbers for this study are discussed.

Section 2.1 The Hydraulic Jump

The hydraulic jump is a phenomenon where shallow, high-velocity flow suddenly converts to deeper, lower-velocity flow. Much of the upstream kinetic energy is lost in the turbulence of the jump. Thus there is less potential for erosion and scour to occur downstream of the jump.

The hydraulic jump was first described by Leonardo da Vinci around the beginning of the sixteenth century. It was not until the nineteenth century, however, that Bidone systematically studied it and Breese wrote the correct formulation of its momentum characteristics.

In 1936 Bakhmeteff and Matzke [1] first analyzed the upstream channel flow conditions in terms of its Froude number

$$F = \frac{V}{(gd)^{1/2}} \dots \dots \dots (2.1.1)$$

where, V is the velocity of flow;

g is the acceleration due to gravity; and

d is the depth normal to flow (rectangular channels).

In 1957 Bradley and Peterka [3] noted five distinct forms of hydraulic jumps in rectangular channels and classified them with respect to their upstream Froude numbers. When the Froude number equals 1.0 the water is flowing at critical depth and no jump can form. For Froude numbers between 1.0 and 1.7 there is only a slight difference in the conjugate depths. For Froude numbers between 1.7 and 2.5 a series of small rollers develop on the surface, and energy loss in the jump is low. For Froude numbers between 2.5 and 4.5 a pulsating action is evident and the jump location can be irregular. In the case of Froude numbers between 4.5 and 9.0 the jump is stable. Energy losses in this jump classification range from 45 to 70 percent. For Froude numbers above 9.0 the difference between conjugate depths is large, and energy losses may reach 85 percent.

In 1964 Silvester [19] provided the exact solutions for the conjugate depths and energy loss for hydraulic jumps in rectangular, triangular, parabolic, circular and trapezoidal channels in terms of the upstream Froude number and showed them to be in agreement with available experimental data. The equation for energy lost in a jump for any channel shape is:

$$\frac{E_L}{E_1} = \frac{\left[2 - \frac{2d_2}{d_1} \right] + F_1^2 \times \left[1 - \frac{A_1^2}{A_2^2} \right]}{\left[2 + F_1^2 \right]} \dots \dots \dots (2.1.2)$$

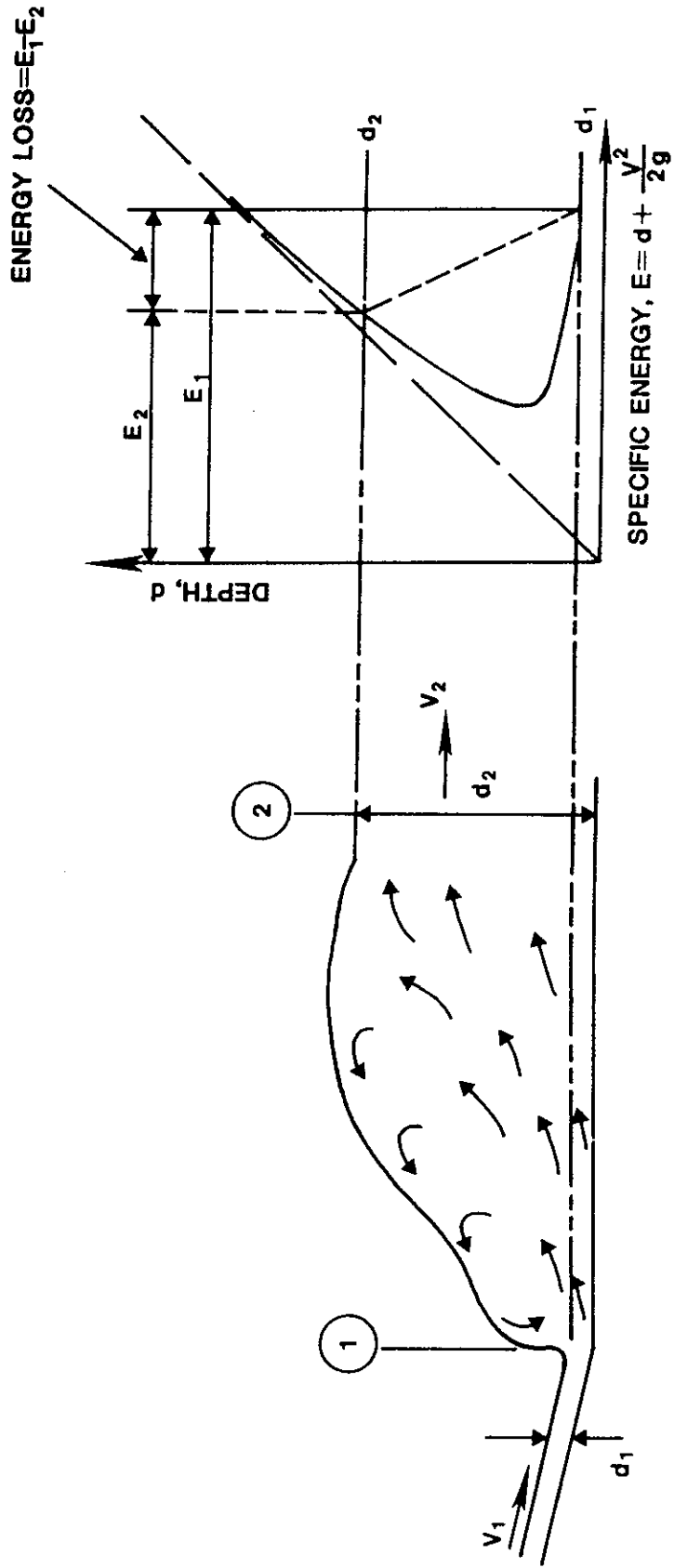


FIGURE 2.1.1 THE HYDRAULIC JUMP

where,

- A_1 is the area of the channel cross section upstream;
- A_2 is the area of the channel cross section downstream;
- d_1 is the depth upstream of the jump;
- d_2 is the depth downstream of the jump;
- E_1 is the energy just upstream of the jump;
- E_L is the energy loss in the jump; and
- F_1 is the upstream Froude number.

Section 2.2 Development of the Ring Chamber

The use of circular roughness elements in culverts on steep slopes and under inlet control, i.e. high energy culverts, was first studied by Wiggert, Erfle and Morris [21,22] in 1972. They placed circular rings inside the periphery of model culverts of constant slope. For the culvert to flow full at the location of the dissipators, four dissipators were needed. The upstream ring was twice the height of the three downstream rings and located twice as far from them as they were from each other (see Figure 2.2.1). The downstream rings were sized and spaced by the following equations:

$$0.06 < K/D < 0.09 \quad \dots \dots \dots (2.2.1)$$

and

$$L/D = 1.5 \quad \dots \dots \dots (2.2.2)$$

where,

- K is the height of the dissipators;
- D is the inside diameter of the culvert; and
- L is the spacing between the three smaller rings.

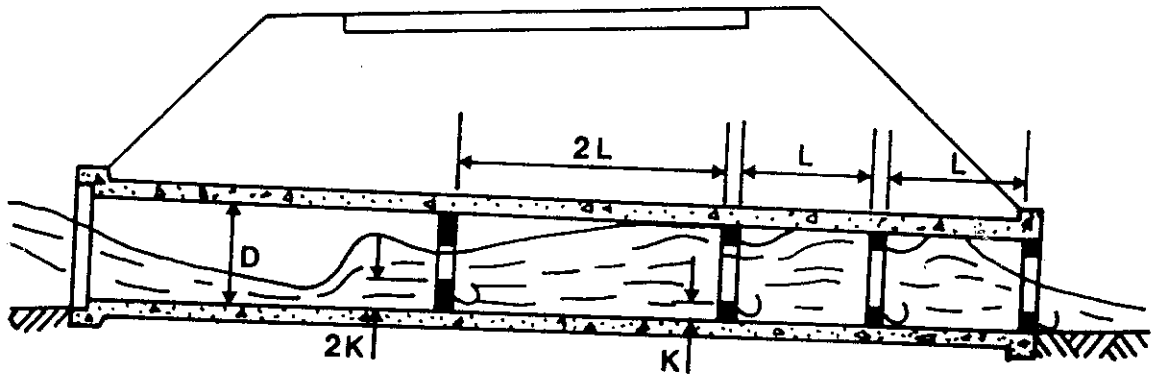


FIGURE 2.2.1 FULL FLOW RING CHAMBER

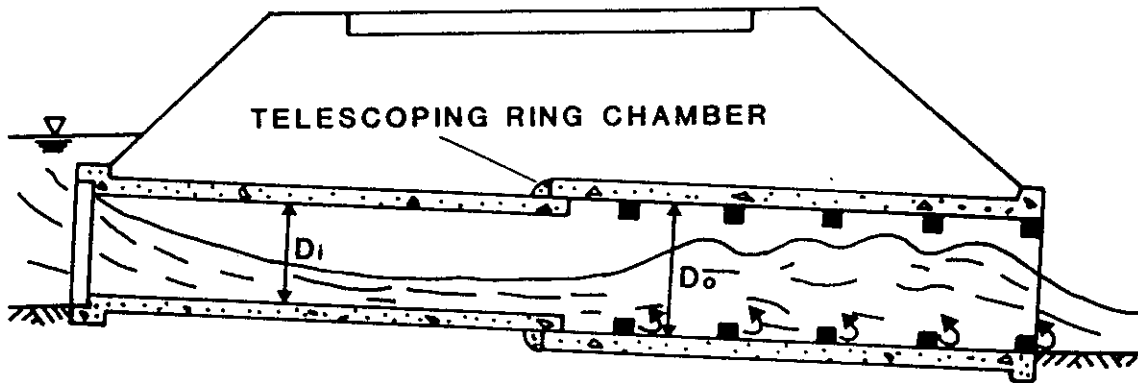


FIGURE 2.2.2 FREE SURFACE FLOW RING CHAMBER

The above researchers also found that by maintaining a free surface throughout the length of a culvert with rings in it, a greater velocity reduction could be achieved than for full flow conditions. This introduced the telescoping ring chamber (see Figure 2.2.2) in which the main section (inlet section) of the culvert is governed by the usual design parameters and the ring chamber diameter is sized by the following equation:

$$\left[\frac{Q^2}{0.10g} \right]^{1/5} < D_0 < \left[\frac{Q^2}{0.044g} \right]^{1/5} \dots \dots \dots (2.2.3)$$

where

Q is the amount of flow in cfs;

g is the acceleration due to gravity; and

D₀ is the inside diameter of the ring chamber pipe in ft.

The above equation requires five rings sized and spaced as follows:

$$0.10 < K/D_0 < 0.15 \dots \dots \dots (2.2.4)$$

and

$$1.5 < L/D_0 < 2.5 \dots \dots \dots (2.2.5)$$

where K, D₀ and L are defined as in Equations (2.2.1), (2.2.2) and (2.2.3).

This design produced a tumbling flow characterized by acceleration between each ring and a hydraulic jump over each ring. Velocity reductions ranged from 50 to 70 percent.

In 1974 the Ohio Department of Transportation (ODOT) designed their first ring chamber using the above equations for free surface flow. The culvert and ring chamber were placed on a 4.4 percent slope. Pettit [16] observed the following on the performance of this type of structure:

"On this structure we discovered the need to reduce the slope of the ring chamber to 0.5% and add a settling distance beyond the last ring station. The steep 4.4% slope established a vertical velocity component that eroded a hole at the outlet beyond the ring chamber. The settling distance provides a solid bottom for the flow section to drop from the top of the ring to the level of the outlet channel. All subsequent ring chambers have been placed on the 0.5% slope (or less)."

ODOT also modified the shape of the rings from a solid ring to two ring segments (see Figure 2.2.3.a). They felt water trapped in front of the solid rings may cause problems during dry periods due to freezing and thawing. The gap, G, at the bottom allows for complete drainage. A gap was included at the top to help the culvert function as an open channel. The upstream edge of the rings also had a 30-degree bevel added to aid in passing debris. All of these changes were substantiated by Sarikelle and Simon [18] of The University of Akron in a report published in 1980.

The value for K (see Figure 2.2.3.b) is one of the hydraulic parameters found in this study. The value for W is based on structural considerations. Hydraulically W should be kept to a minimum but structurally it should be wide enough to allow for reinforcing bars to be placed in the dissipators to protect them from damaging collisions from passing debris. Values of K and W in terms of D_0 can be found in Table 5.3.1.

ODOT later modified the ring dissipators from a 2-piece to a 4-piece design to further simplify their construction and placement into the ring chamber (see Figures 2.2.3.a and 2.2.4).

This study found that the 4-piece design could be modified to a new 2-piece design (see Figure 2.2.5) and still cause hydraulic jumps to form in the ring chamber.

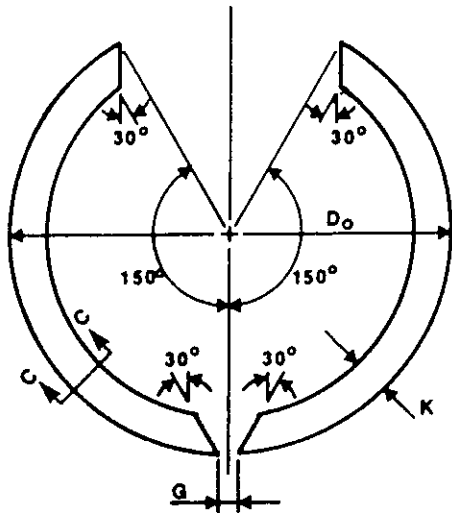
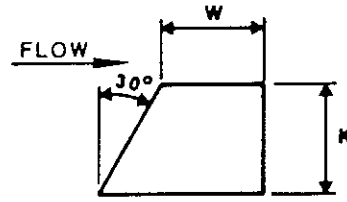


FIGURE 2.2.3.a OLD 2-PIECE DISSIPATOR



SECTION C-C

FIGURE 2.2.3.b SECTION C-C

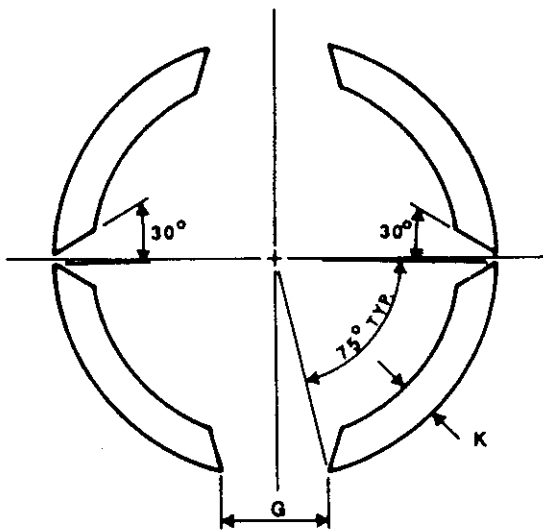


FIGURE 2.2.4 4-PIECE DISSIPATOR

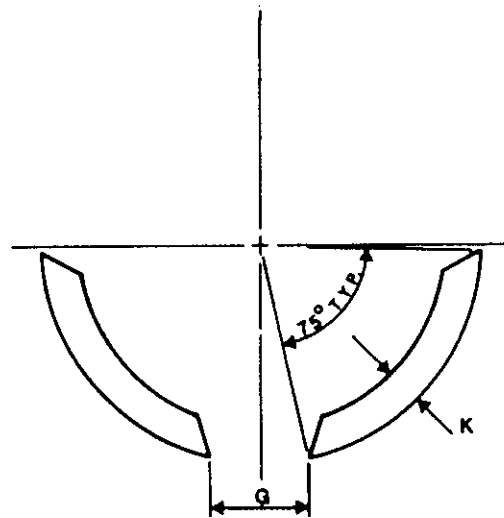


FIGURE 2.2.5 NEW 2-PIECE DISSIPATOR

Section 2.3 Hydraulic Modeling for this Study

Most hydraulics texts (see References [5,10,11,13,20]) derive the equations and show the relationships that must be followed between the small-scale model and the prototype for the model to predict the performances of the prototype.

For a model to give exact calculations as to how a prototype would work, all forces present in the prototype must be modeled. This is impossible so usually the single, dominant force is modeled and the results are calibrated with similar or related prototype performances.

This study is basically an open-channel flow problem, therefore, gravity is the single most dominant force effecting the performance of the prototype. The important equation describing gravity flow is the Froude number

$$\frac{V}{(gL')^{1/2}} \quad (2.3.1)$$

where L' presents the hydraulic depth (see Section 2.4).

The relationship to be followed is the Froude modeling law. It states that the Froude number at any point in the model must equal the Froude number at the corresponding point in the prototype.

The results obtained from following Equation (2.3.1) and the Froude modeling law are reported in Chapter 4 and calibrated in Chapter 5.

Section 2.4 Froude Numbers for this Study

In the Froude number Equation (2.3.1), L' represents a characteristic length which for open-channel flow is the hydraulic depth. This is defined as the area of flow normal to the flow's direction divided by the top width of the flow's free surface. For rectangular channels this is

simply the depth of flow, d . For circular channels the hydraulic depth is a more complicated calculation. To simplify Froude number calculations for circular channels in this study the hydraulic depth has been replaced by the actual depth, d .

For those interested, the true Froude number for a circular channel flowing less than half-full can be approximated using the equation below:

$$F' = 1.135 F^{1.019} \quad (2.4.1)$$

where F' is the true Froude number calculated with the hydraulic depth and F is the Froude number calculated with the actual depth.

CHAPTER 3
EXPERIMENTAL SETUP

This chapter gives a brief description of equipment used and tests run to obtain the results reported in Chapter 4.

Section 3.1 Equipment

An adjustable-slope flume was used with a 32.8 ft. (10.0m) long glass-sided channel with a cross section of 11.8 in. by 11.8 in. (0.3m by 0.3m). At one end, a headbox was built with a 4.0-in. diameter (all diameters are inside diameters) pipe-stub jutting out. A 6.0-in. clear acrylic pipe was connected to the stub which was in turn connected to a joint with rubber sleeves that could accommodate either a 4.0-in., 4.75-in., 5.50-in. or 6.0-in. clear acrylic pipe (see Figure 3.1.1). The latter served as a model of an inlet pipe. The inlet was connected to a model of the ring chamber.

The ring chamber was made of 1.25-in., 3.0-in. and 6.0-in. lengths of 6.0-in. clear acrylic pipe segments taped together with clear weather-stripping tape. Roughness elements were molded into the 1.25-in. segments before taping to form models of the dissipators used by ODOT. There were 2-piece and 4-piece dissipators with heights, K , of 0.5-in., 0.75-in. and 1.0-in. This gave relative heights, K/D_0 , of 1/12, 1/8 and 1/6 respectively. Holes were drilled in the inlet pipes and some of the pipe segments so that the depth of flow could be measured with a point gage. The ring chamber was set on an aluminum channel to align the segments on the bottom of the flume's channel. A 15-hp pump was used that could deliver up to 1.25 cfs (35.4 l/s) of flow. The pump's discharge was measured with a rotameter.

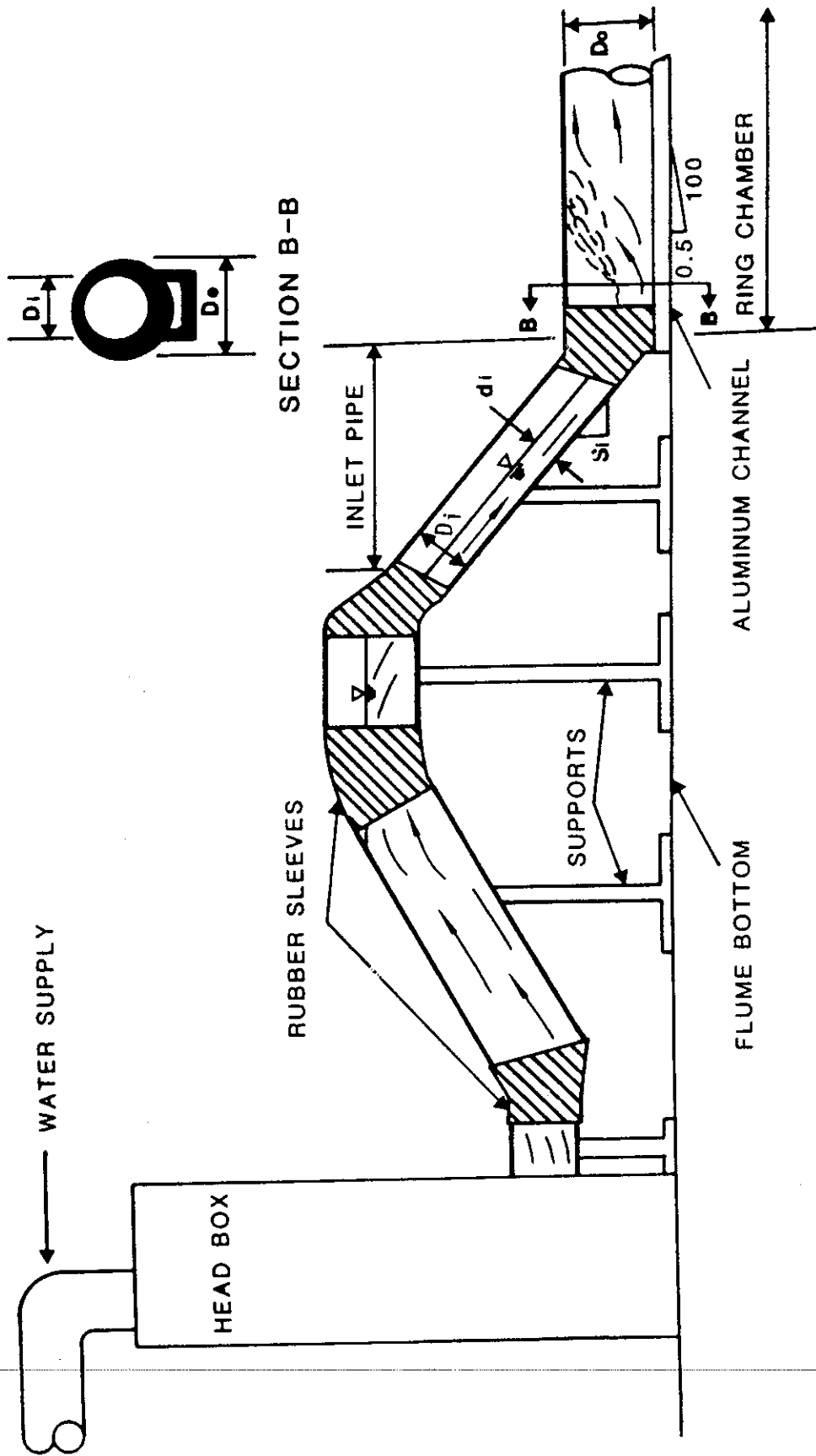


FIGURE 3.1.1 EXPERIMENTAL SETUP

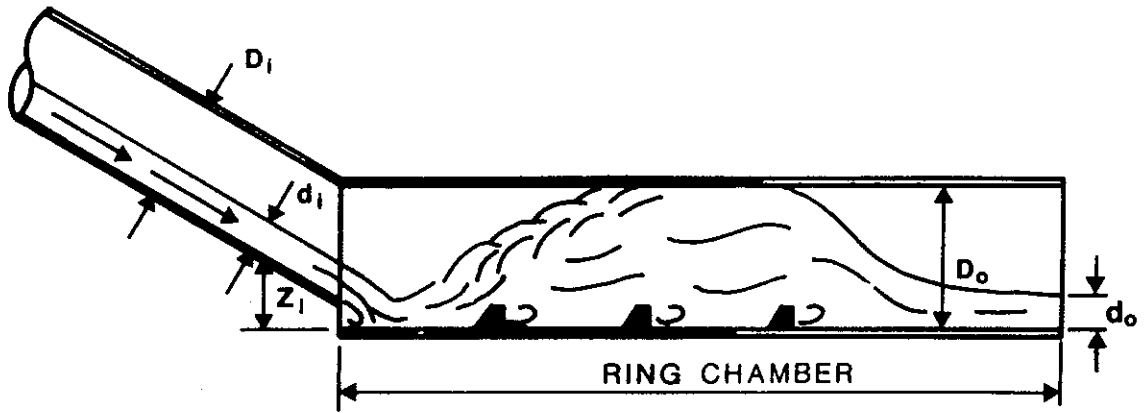


FIGURE 3.2.1 RING CHAMBER FLOWING JUST FULL

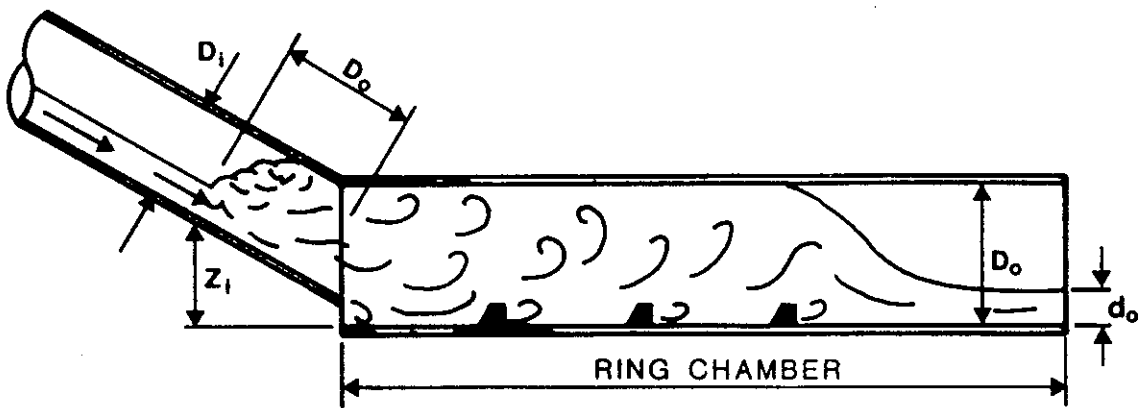


FIGURE 3.2.2 RING CHAMBER FLOWING FULLY CHOKED

where, V_i is the velocity in the inlet;

d_i is the depth of water in the inlet pipe; and

Z_i is the elevation of the pipe inlet where d_i is measured (Z_i was measured relative to the outlet being at zero elevation).

Similarly, the energy of flow at the outlet was found by

$$E_o = \frac{V_o^2}{2g} + d_o \dots \dots \dots (3.2.2)$$

The percent energy lost in the ring chamber is

$$E_L = \left[\frac{E_i - E_o}{E_i} \right] \times 100 \dots \dots \dots (3.2.3)$$

All the above tests were done with the ring chamber on a slope of 0.005 ft/ft because this simulates the designs undertaken by ODOT. In the preliminary tests the slope of the ring chamber was adjusted within a range of 0.002 ft/ft to 0.025 ft/ft. The effect of these changes were found to be relatively minor and, therefore, it was not considered to be a significant hydraulic variable.

CHAPTER 4

RESULTS

This chapter gives the results obtained from three sets of model tests. The first set is for four 2-piece dissipators with $L/D_0 = 1.0$, $K/D_0 = 1/8$ and with the ring chamber just full. The second set is for the same conditions as the first set except the ring chamber was fully choked with the hydraulic jump occurring one ring-chamber-diameter distance into the inlet pipe. The third set is for three 2-piece dissipators with $L/D_0 = 1.0$, $K/D_0 = 1/6$ and with the ring chamber fully choked as above.

The graphs shown herein represent the data from the above tests as listed in Tables 4.1.1.a. to 4.1.1.c. The first section is on Figures 4.1.1 to 4.1.9. The second section is on energy reduction graphs, Figures 4.2.1 and 4.2.2. The third section is on velocity reductions graphs, Figures 4.3.1 and 4.3.2.

Section 4.1 Figures 4.1.1 to 4.1.9

Figures 4.1.1 to 4.1.9 give the inlet Froude number (2.1.1) (found where d_i and Z_i are on Figure 3.2.1) and the inlet relative depth (depth normal to flow divided by the inside diameter of the inlet - d_i/D_i) necessary to cause certain flow conditions in the ring chamber. For instance, on Figure 4.1.1 the lowest line represents the best-fit through data points taken from tests where $L/D_0 = 1.0$, $K/D_0 = 1/8$ and where the ring chamber diameter was the same size as the inlet pipe ($D_0/D_i = 1.000$) and the flow was just full. Any point on this line gives the inlet Froude number and the inlet relative depth necessary to cause the given ring chamber to flow just full. Any point below this implies that for that Froude number and relative depth the given ring chamber would flow

TABLE 4.1.1.1.a DATA FOR JUST-FULL CONDITIONS; 4 DISSIPATORS; $L/D_0 = 1.0$; $K/D_0 = 1/8$

D_0/D_i	Inlet Slope (Degrees)	Flow (CFS)	Inlet Velocity (ft/s)	Inlet Froude Number	d_i/D_i	Outlet Froude Number	Velocity Reduction %	Energy Reduction %
1.000	28.9	0.276	10.57	6.04	0.19	1.54	63.50	78.71
1.000	24.7	0.276	8.81	4.72	0.22	1.47	57.62	71.70
1.000	21.0	0.282	9.19	4.96	0.21	1.50	58.44	72.77
1.000	17.7	0.263	8.59	4.64	0.21	1.44	57.72	71.21
1.000	14.1	0.339	7.52	3.54	0.28	1.63	43.39	57.02
1.000	10.6	0.339	6.76	3.06	0.30	1.60	37.77	49.46
1.000	7.1	0.378	6.01	2.51	0.36	1.61	27.49	36.99
1.000	3.7	0.384	7.35	3.28	0.31	1.81	35.24	46.92
1.091	30.2	0.263	11.31	6.61	0.20	1.40	68.52	82.97
1.091	27.2	0.263	9.48	5.21	0.22	1.40	62.46	77.12
1.091	23.9	0.256	9.13	4.99	0.23	1.42	60.91	75.60
1.091	18.9	0.320	9.75	5.05	0.25	1.57	58.03	73.65
1.091	15.4	0.339	7.23	3.29	0.33	1.56	42.93	57.57
1.091	11.5	0.327	6.99	3.19	0.33	1.56	41.41	55.05
1.091	7.8	0.352	5.97	2.50	0.39	1.69	26.06	39.33
1.091	4.0	0.378	5.65	2.26	0.43	1.61	22.87	33.57
1.091	6.2	0.403	5.25	1.99	0.47	1.63	14.84	25.69
1.263	23.3	0.244	11.32	6.60	0.23	1.43	68.78	83.64
1.263	20.8	0.244	9.93	5.53	0.25	1.45	63.91	79.41
1.263	17.6	0.263	8.14	4.10	0.31	1.48	54.44	70.71
1.263	14.9	0.263	8.11	4.09	0.31	1.43	55.53	70.89
1.263	10.5	0.327	7.80	3.58	0.37	1.51	48.76	64.22
1.263	7.9	0.333	6.79	2.93	0.42	1.57	39.20	55.35
1.263	5.4	0.352	6.25	2.56	0.47	1.64	30.64	47.67
1.263	5.5	0.378	5.81	2.25	0.52	1.67	23.22	39.39
1.500	29.2	0.260	9.88	5.16	0.34	1.46	62.93	79.28
1.500	24.1	0.256	9.89	5.19	0.34	1.42	63.92	79.53
1.500	19.8	0.279	9.76	4.95	0.36	1.46	61.83	77.81
1.500	16.8	0.359	9.61	4.41	0.44	1.62	55.16	72.62
1.500	13.3	0.368	8.82	3.87	0.48	1.57	51.83	68.76

TABLE 4.1.1.1.b DATA FOR FULLY-CHOKED CONDITIONS; 4 DISSIPATORS; $L/D_0 = 1.0$; $K/D_0 = 1/8$

D_0/D_i	Inlet Slope (Degrees)	Flow (cfs)	Inlet Velocity (ft/s)	Inlet Froude Number	d_i/D_i	Outlet Froude Number	Velocity Reduction %	Energy Reduction %
1.000	24.7	0.378	9.74	4.84	0.25	1.89	49.80	67.09
1.000	17.7	0.454	9.16	4.17	0.30	1.58	50.75	64.26
1.000	14.1	0.461	7.61	3.22	0.35	1.61	39.52	51.33
1.000	10.6	0.454	7.08	2.93	0.36	1.63	34.58	45.33
1.000	7.1	0.454	6.76	2.76	0.37	1.64	31.23	40.66
1.000	3.7	0.416	7.02	2.99	0.34	1.66	34.95	44.46
1.091	30.2	0.288	10.29	5.63	0.23	1.42	64.20	79.04
1.091	27.2	0.343	9.89	5.02	0.26	1.60	57.34	73.79
1.091	23.9	0.365	9.16	4.43	0.29	1.62	52.69	68.99
1.091	18.9	0.365	9.32	4.53	0.29	1.58	54.32	69.71
1.091	11.5	0.359	6.86	3.00	0.35	1.65	36.38	50.50
1.091	7.8	0.403	6.14	2.47	0.42	1.63	27.16	39.27
1.091	4.0	0.429	5.68	2.16	0.47	1.59	21.48	31.48
1.263	23.3	0.295	12.41	6.98	0.25	1.41	70.21	84.60
1.263	20.8	0.320	10.23	5.22	0.30	1.55	60.49	76.72
1.263	17.6	0.327	9.01	4.36	0.34	1.55	54.82	71.23
1.263	14.9	0.339	8.24	3.80	0.37	1.57	49.59	66.13

TABLE 4.1.1.1.c DATA FOR FULLY-CHOKED CONDITIONS; 3 DISSIPATORS; $L/D_0 = 1.0$; $K/D_0 = 1/6$

D_0/D_i	Inlet Slope (Degrees)	Flow (cfs)	Inlet Velocity (ft/s)	Inlet Froude Number	d_i/D_i	Outlet Froude Number	Velocity Reduction %	Energy Reduction %
1.000	29.5	0.314	12.17	6.98	0.19	1.47	68.24	82.47
1.000	25.6	0.307	10.05	5.43	0.21	1.52	60.68	75.28
1.000	21.3	0.339	8.87	4.43	0.25	1.60	52.60	67.51
1.000	18.3	0.349	9.77	5.00	0.24	1.62	56.30	71.36
1.000	10.6	0.448	7.53	3.21	0.34	1.69	37.13	49.48
1.000	3.7	0.480	6.14	2.36	0.42	1.68	21.92	29.15
1.091	27.9	0.279	11.19	6.39	0.21	1.43	67.14	81.43
1.091	24.9	0.279	10.20	5.63	0.22	1.43	63.95	78.09
1.091	19.4	0.323	8.65	4.27	0.28	1.49	54.51	68.80
1.091	15.4	0.391	8.34	3.80	0.33	1.58	48.09	61.93
1.091	11.3	0.406	7.46	3.22	0.37	1.62	40.23	53.11
1.091	4.1	0.429	6.83	2.79	0.41	1.62	33.67	43.74
1.263	20.3	0.307	10.48	5.47	0.29	1.49	62.99	78.51
1.263	18.0	0.346	9.29	4.45	0.34	1.64	53.63	70.59
1.263	15.1	0.387	8.70	3.90	0.39	1.51	51.98	67.06
1.263	11.6	0.429	8.23	3.48	0.44	1.60	45.56	61.05
1.500	29.2	0.269	9.66	4.94	0.36	1.37	63.47	79.17
1.500	25.9	0.266	9.30	4.71	0.36	1.46	60.48	77.12
1.500	21.2	0.333	9.72	4.61	0.42	1.52	58.57	75.32
1.500	18.9	0.371	9.39	4.22	0.46	1.35	59.32	73.87
1.500	14.6	0.400	9.04	3.88	0.51	1.38	56.28	70.91
1.500	12.7	0.419	8.37	3.42	0.56	1.37	52.35	67.13

less than just full. Similarly, any point above this line implies that for that Froude number and relative depth the given ring chamber would flow more than just full.

The next line gives the inlet Froude numbers and inlet relative depths for just full conditions when the ring chamber diameter is 1.091 times larger than the inlet pipe diameter, etc.

The only difference between Figure 4.1.1 and Figure 4.1.2 is that the latter represents choked conditions. Figures 4.1.3 - 4.1.5 compare individual lines from Figures 4.1.1 and 4.1.2 that have the same value for D_o/D_i . They show how choking conditions allow for larger inlet Froude numbers and inlet relative depths than just full conditions for a given value of D_o/D_i .

Figure 4.1.6 is for fully choked conditions but with a shorter ring chamber with fewer but larger dissipators; i.e., three 2-piece dissipators with $L/D_o = 1.0$ and $K/D_o = 1/6$.

Figures 4.1.7 to 4.1.9 compare individual lines from Figures 4.1.2 and 4.1.6 that have the same value for D_o/D_i . The closeness of these lines shows that for fully choked conditions there is little difference in the performance of ring chambers where there are four dissipators with $K/D_o = 1/8$ or three dissipators with $K/D_o = 1/6$.

Table 4.1.2 gives the best-fit equation for each line in Figures 4.1.1, 4.1.2 and 4.1.6.

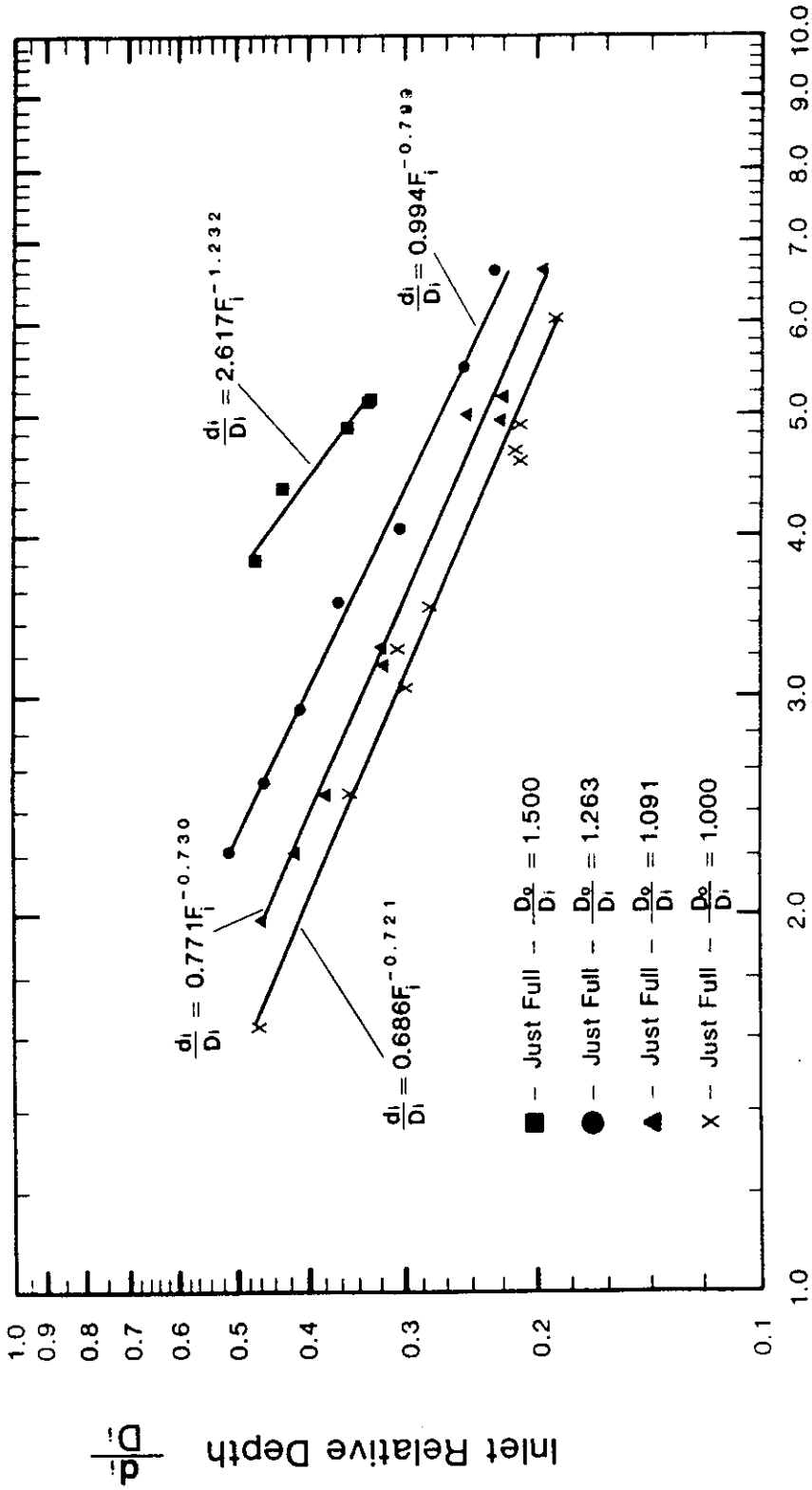


FIGURE 4.1.1.1 PERFORMANCE GRAPH FOR JUST-FULL CONDITION; 4 DISSIPATORS; $L/D_o = 1.0$; $K/D_o = 1/8$

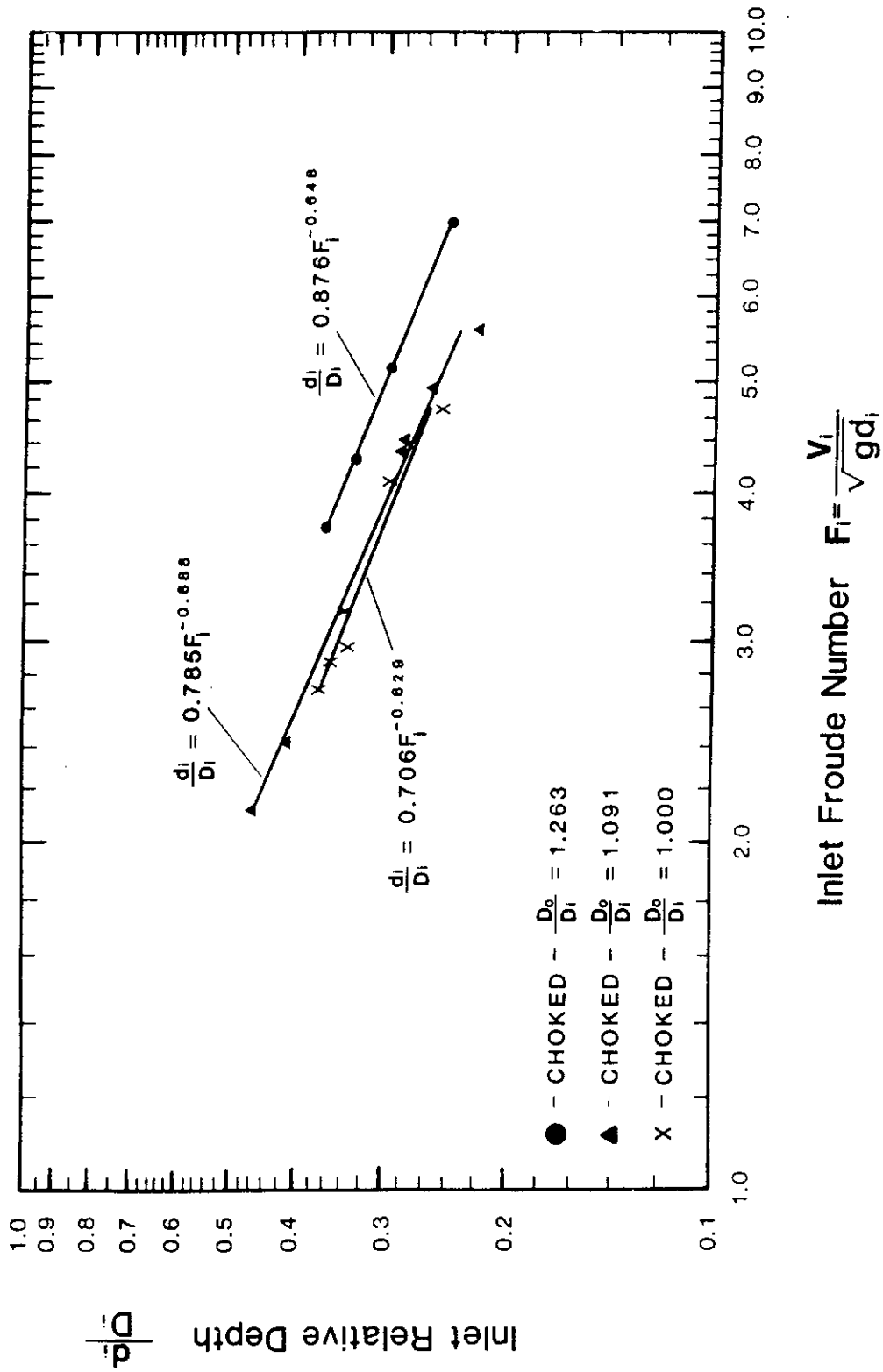


FIGURE 4.1.2 PERFORMANCE GRAPH FOR FULLY-CHOKED CONDITIONS; 4 DISSIPATORS; $L/D_0 = 1.0$; $K/D_0 = 1/8$

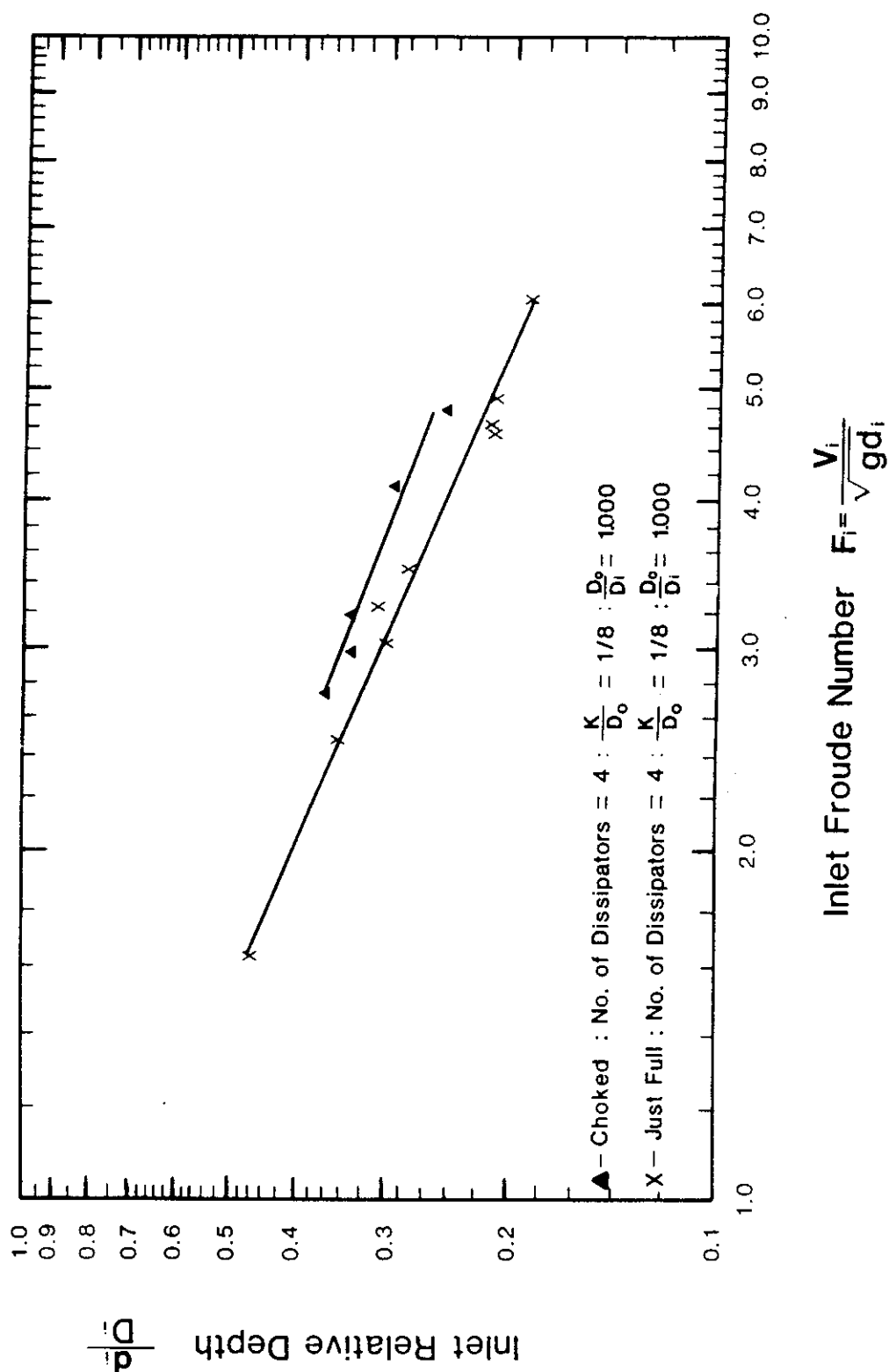


FIGURE 4.1.3 COMPARISON OF FIGURES 4.1.1 and 4.1.2 at $D_o/D_i = 1.000$

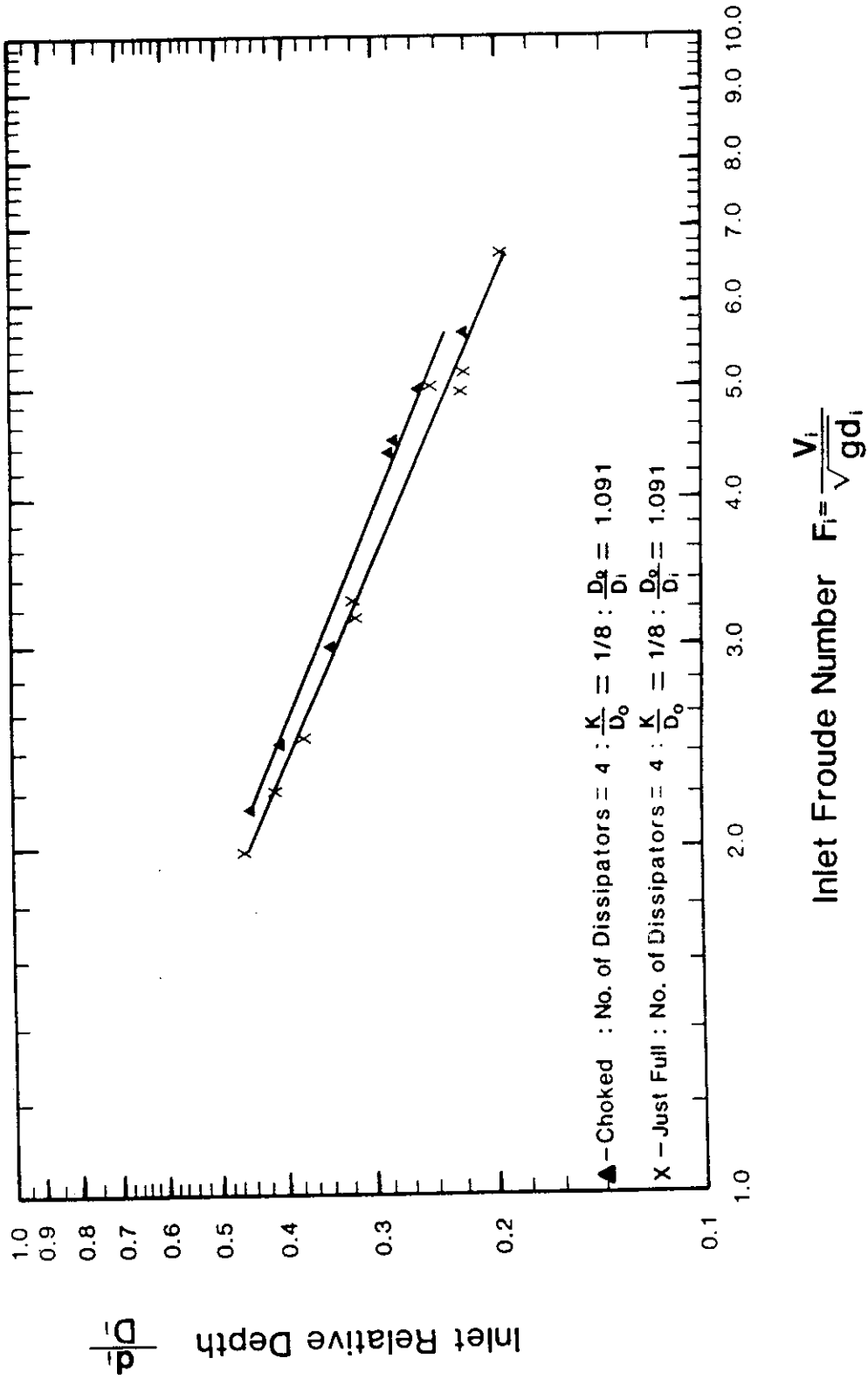


FIGURE 4.1.4 COMPARISON OF FIGURES 4.1.1 and 4.1.2 at $D_0/D_1 = 1.091$

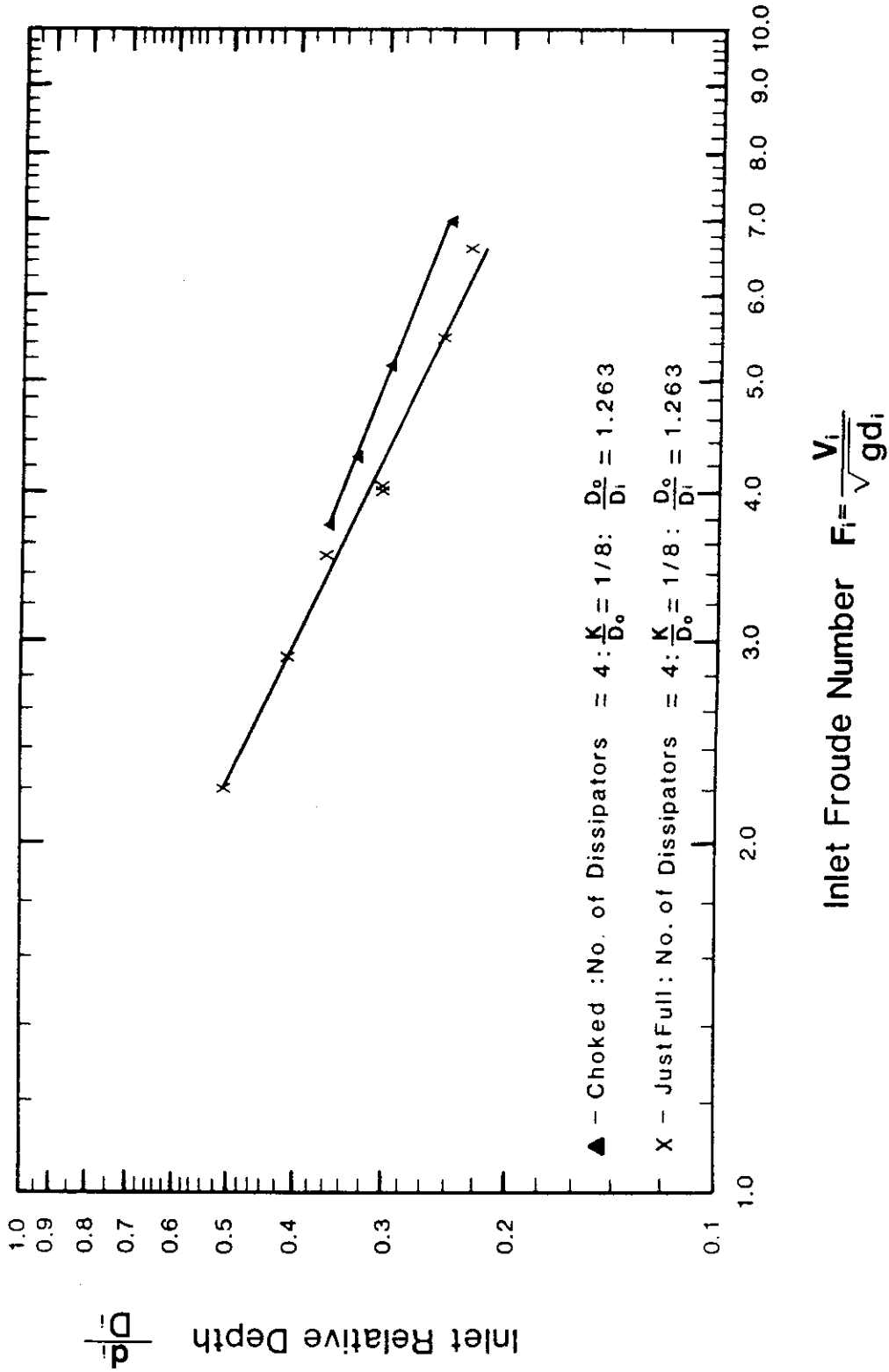


FIGURE 4.1.5 COMPARISON OF FIGURES 4.1.1 and 4.1.2 at $D_o/D_i = 1.263$

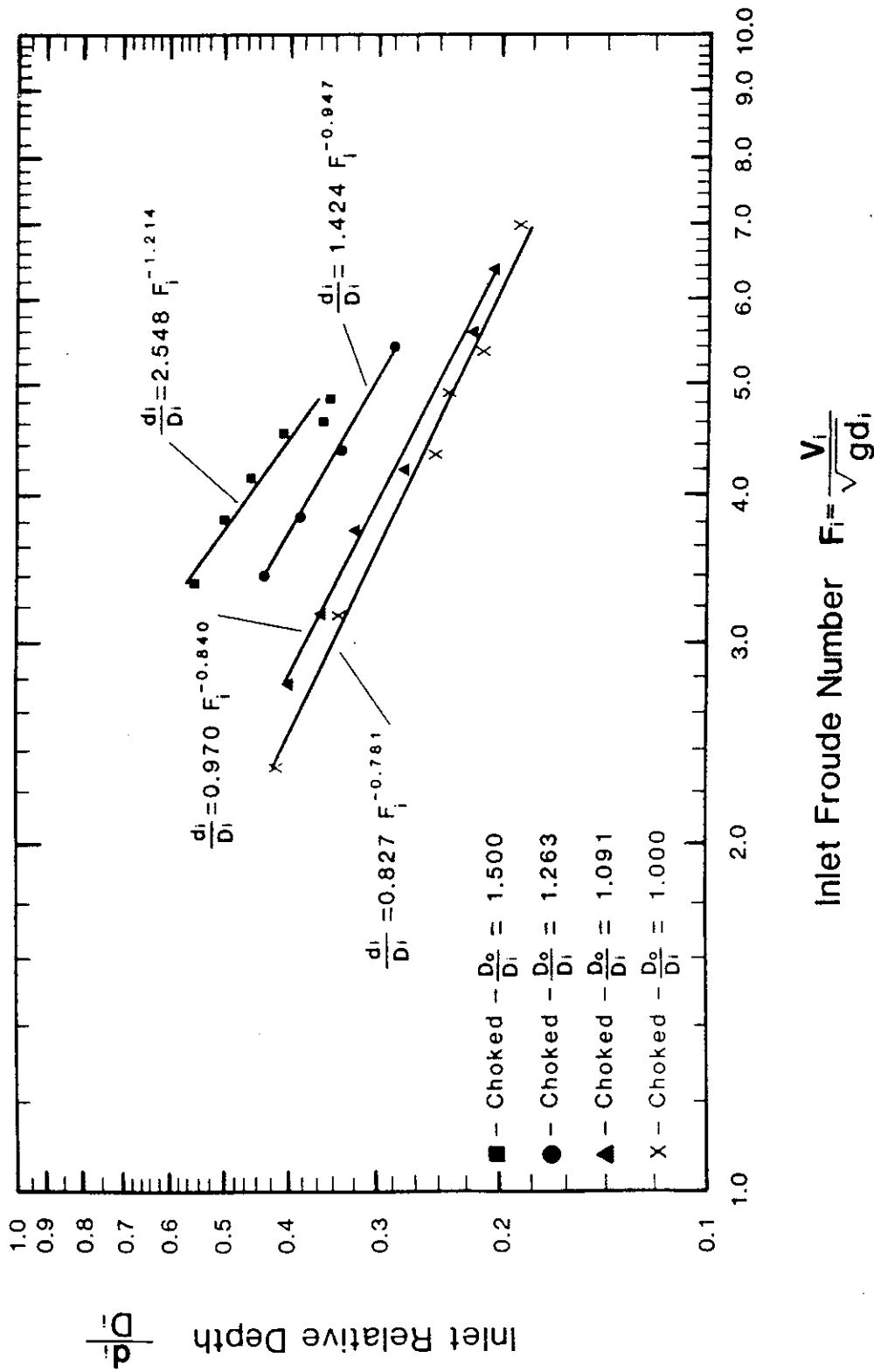


FIGURE 4.1.6 PERFORMANCE GRAPH FOR FULLY-CHOKED CONDITIONS; 3 DISSIPATORS; $L/D_0 = 1.0$; $K/D_0 = 1/6$

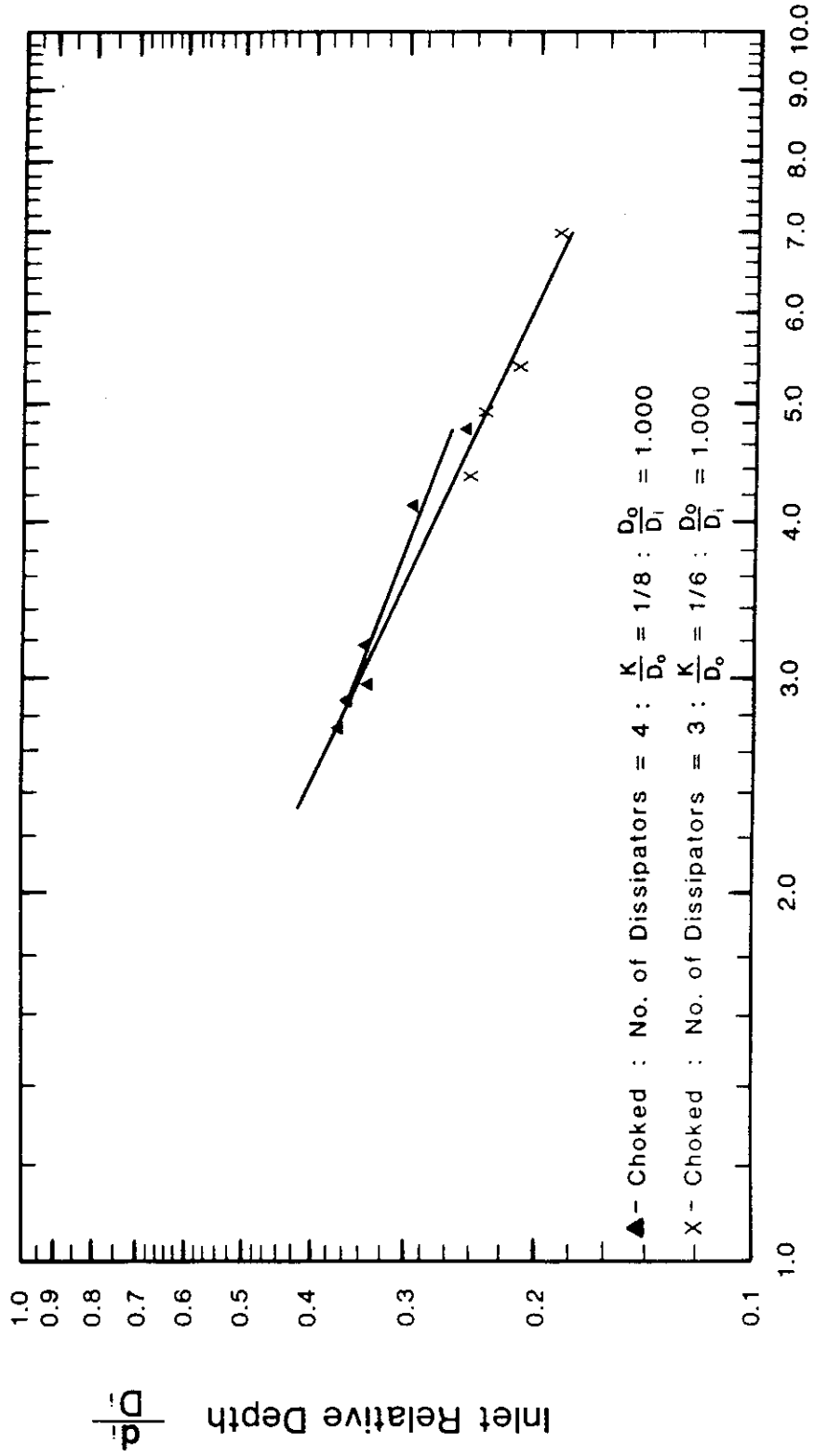


FIGURE 4.1.7 COMPARISON OF FIGURES 4.1.2 and 4.1.6 at $D_o/D_i = 1.000$

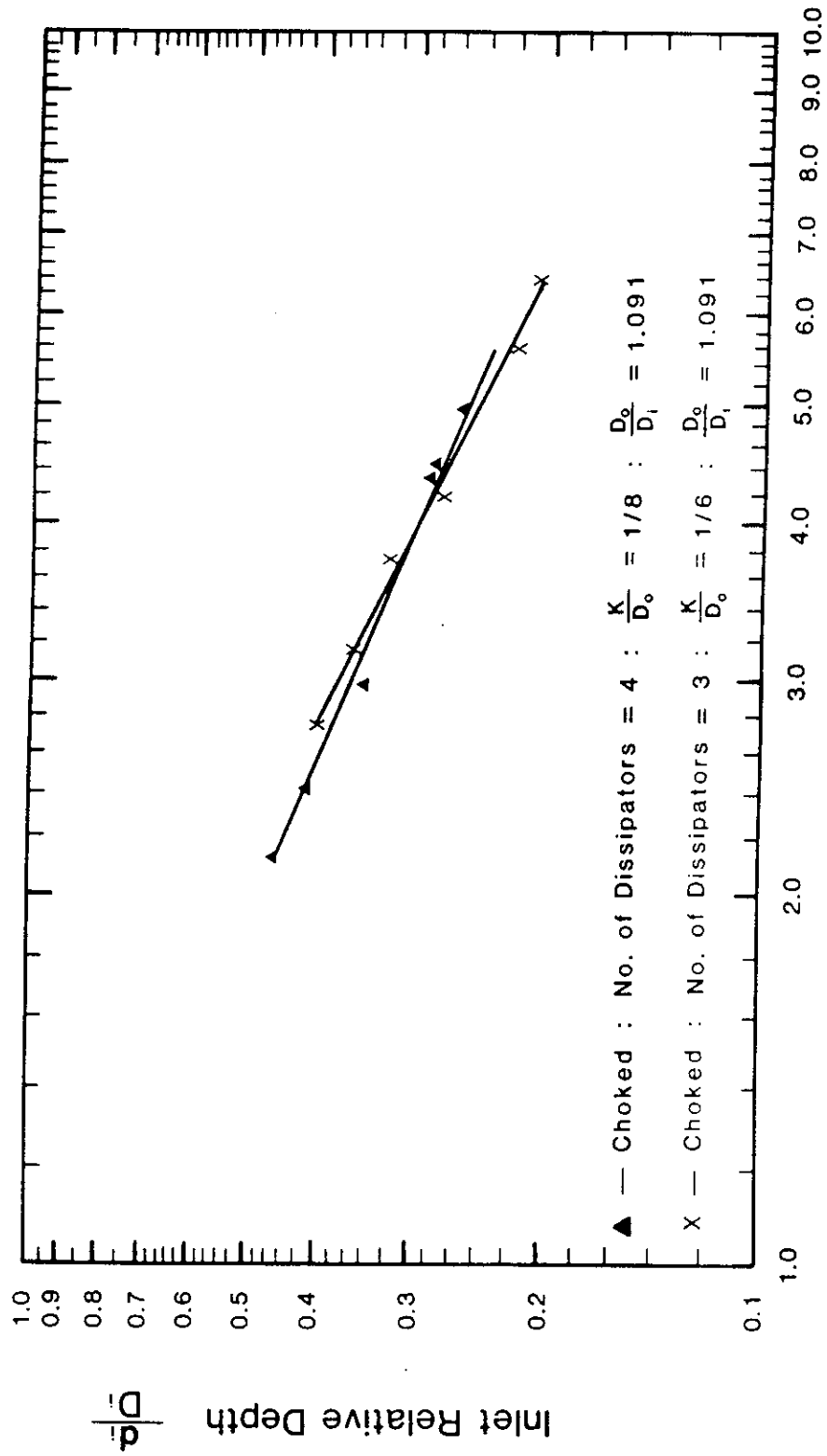


FIGURE 4.1.8 COMPARISON OF FIGURES 4.1.2 AND 4.1.6 at $D_0/D_i = 1.091$

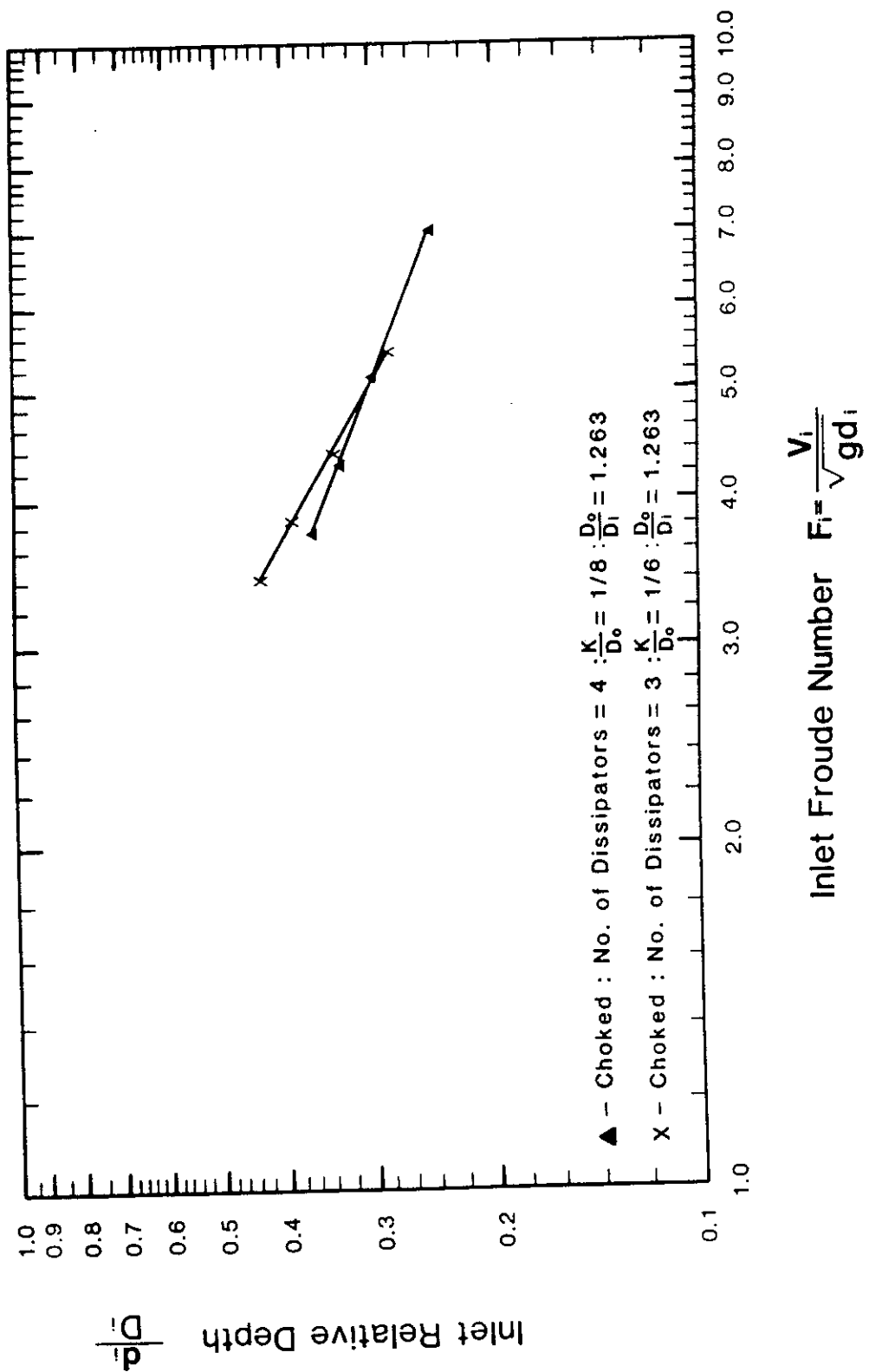


FIGURE 4.1.9 COMPARISON OF FIGURES 4.1.2 and 4.1.6 at $D_0/D_i = 1.263$

TABLE 4.1.2 BEST-FIT EQUATIONS FOR FIGURES 4.1.1, 4.1.2 and 4.1.6

JUST FULL: NO. OF DISSIPATORS = 4 : L/D ₀ = 1.0 : K/D ₀ = 1/8	
$\frac{D_0}{D_i}$	EQUATION
1.000	$\frac{d_i}{D_i} = 0.686 F_i^{-0.721}$
1.091	$\frac{d_i}{D_i} = 0.771 F_i^{-0.730}$
1.263	$\frac{d_i}{D_i} = 0.994 F_i^{-0.799}$
1.500	$\frac{d_i}{D_i} = 2.617 F_i^{-1.232}$
=====	
CHOKED : NO. OF DISSIPATORS = 4 : L/D ₀ = 1.0 : K/D ₀ = 1/8	
1.000	$\frac{d_i}{D_i} = 0.706 F_i^{-0.629}$
1.091	$\frac{d_i}{D_i} = 0.785 F_i^{-0.688}$
1.263	$\frac{d_i}{D_i} = 0.876 F_i^{-0.648}$
=====	
CHOKED : NO. OF DISSIPATORS = 3 : L/D ₀ = 1.0 : K/D ₀ = 1/6	
1.000	$\frac{d_i}{D_i} = 0.827 F_i^{-0.781}$
1.091	$\frac{d_i}{D_i} = 0.970 F_i^{-0.840}$
1.263	$\frac{d_i}{D_i} = 1.424 F_i^{-0.947}$
1.500	$\frac{d_i}{D_i} = 2.548 F_i^{-1.214}$

Section 4.2 Energy Reduction Graphs

Figure 4.2.1 shows percent energy reduction, E_{RED} , as a function of the inlet Froude number. All inlet relative depth values tested are represented. It is observed that there is close agreement between all three best-fit lines.

Figure 4.2.2 shows the single best-fit line for energy reduction for all three sets of tests. The equation for this line is

$$\%E_{RED} = 160.3[\ln(F_i)]^{0.347} - 114.8 \dots \dots (4.2.1)$$

where $\ln(F_i)$ indicates to take the natural logarithm of the inlet Froude number, F_i .

Section 4.3 Velocity Reduction Graphs

Figure 4.3.1 shows the percent velocity reduction, V_{RED} , as a function of the inlet Froude number. All inlet relative depth values tested are represented here. It is again observed that there is close agreement between all three best-fit lines.

Figure 4.3.2 shows the single best-fit line for velocity reduction for all three sets of tests. The equation for this line is

$$\% V_{RED} = 127.4 [\ln(F_i)]^{0.395} - 94.6 \dots \dots (4.3.1)$$

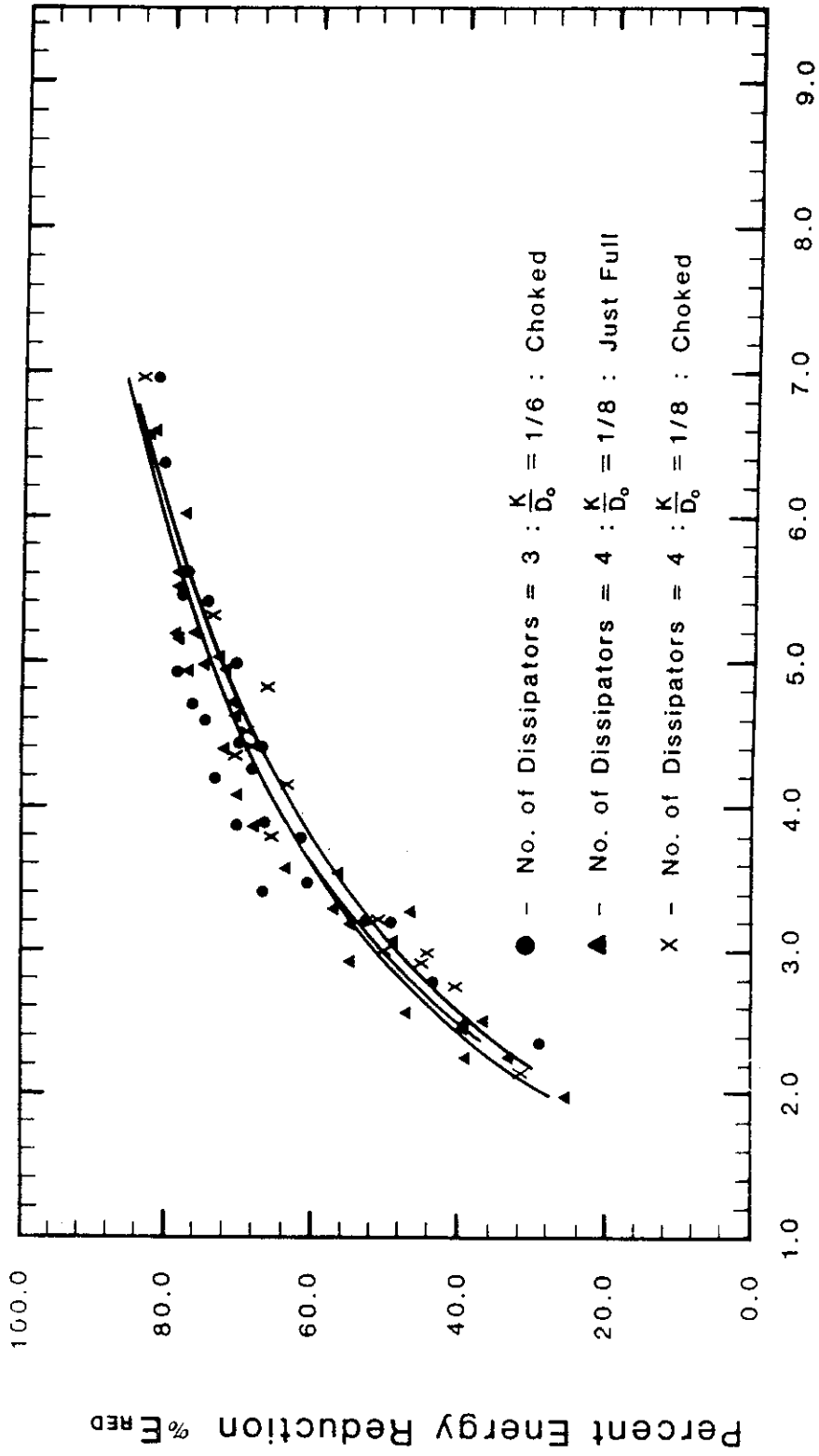


FIGURE 4.2.1 BEST-FIT CURVES FOR PERCENT ENERGY REDUCTION

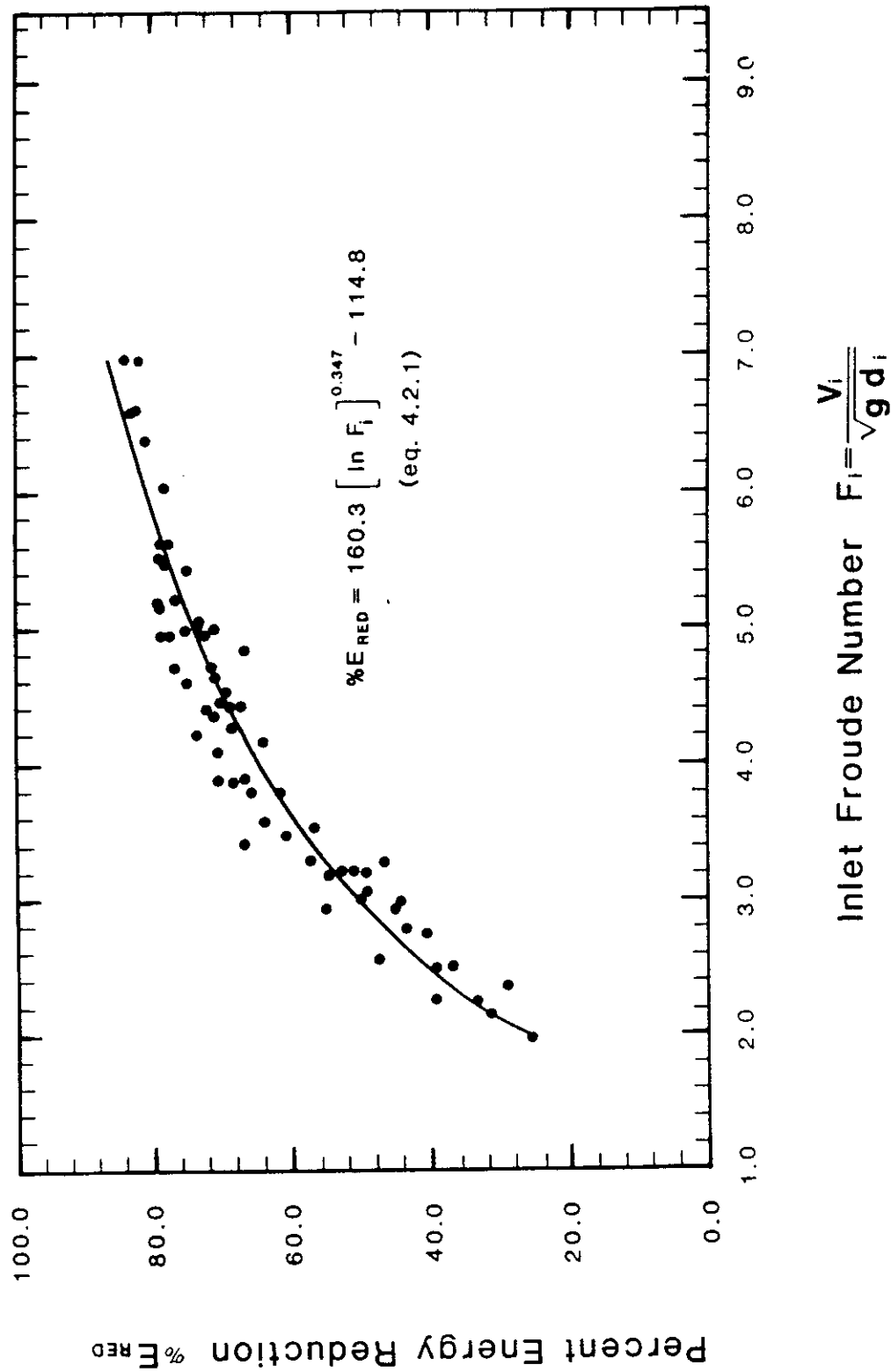
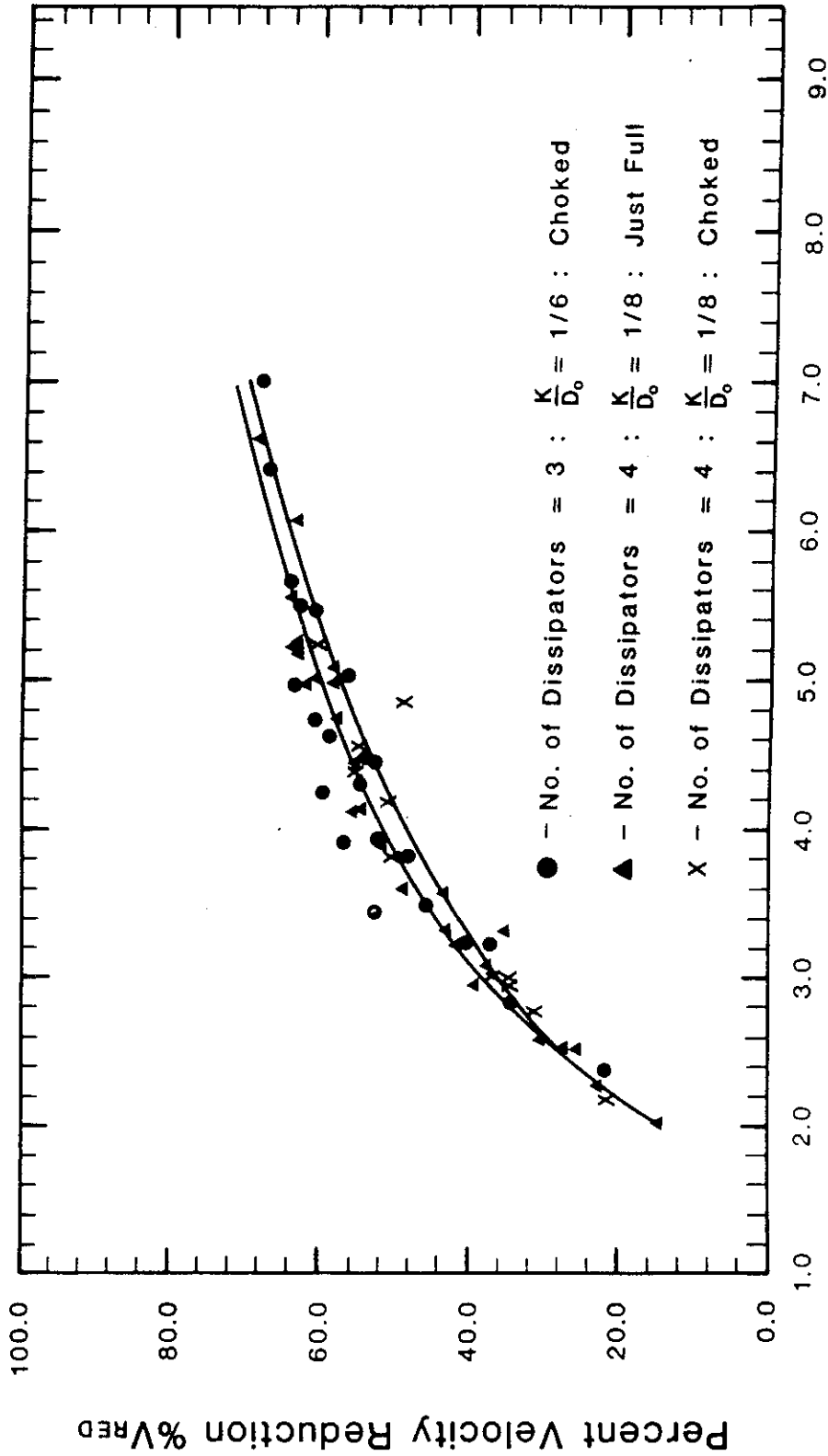
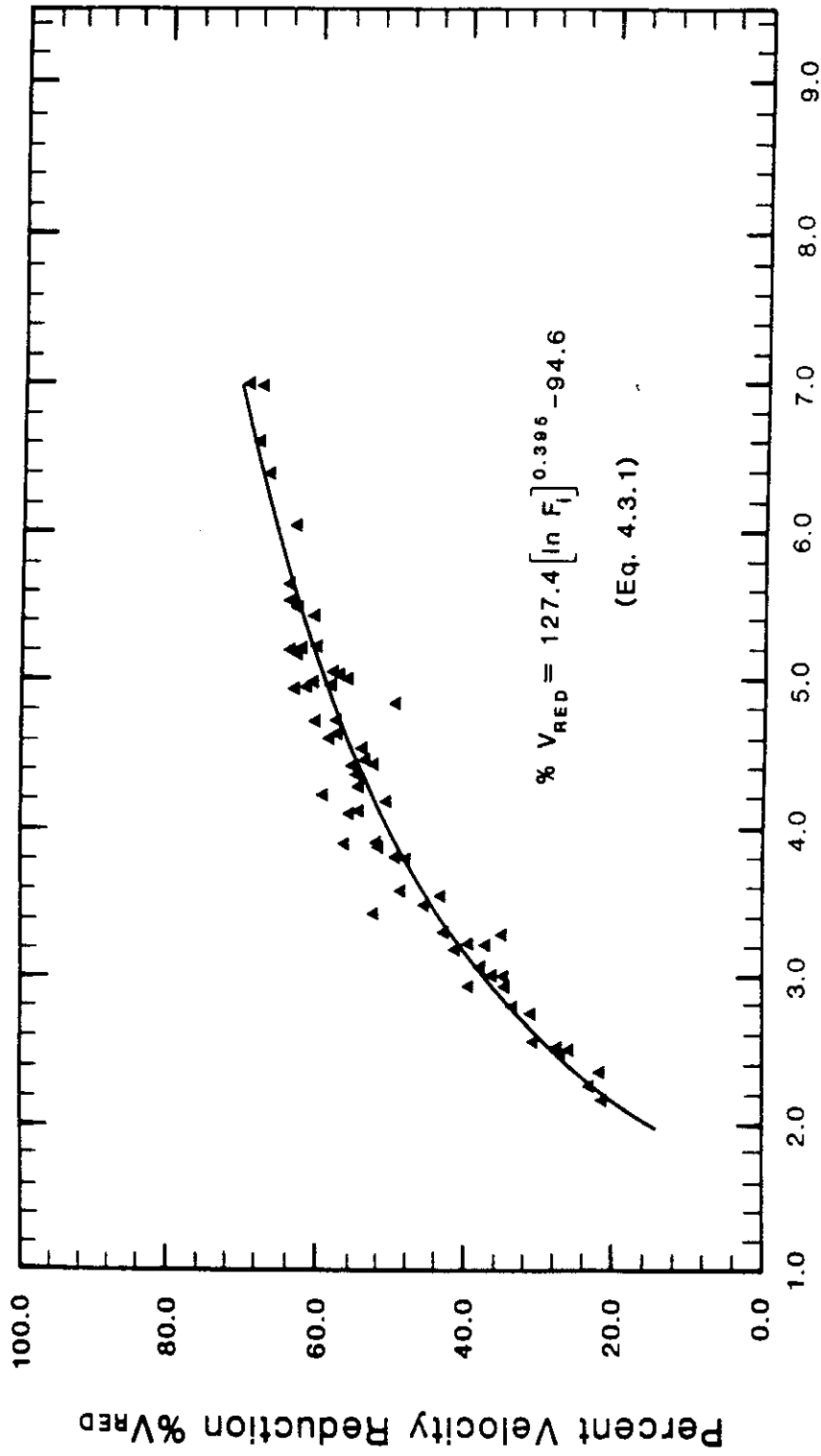


FIGURE 4.2.2 BEST-FIT CURVE FOR PERCENT ENERGY REDUCTION



$$\text{Inlet Froude Number } F_i = \frac{V_i}{\sqrt{g d_i}}$$

FIGURE 4.3.1 BEST-FIT CURVES FOR PERCENT VELOCITY REDUCTION



$$\text{Inlet Froude Number } F_i = \frac{V_i}{\sqrt{g d_i}}$$

FIGURE 4.3.2 BEST-FIT CURVE FOR PERCENT VELOCITY REDUCTION

CHAPTER 5

CONCLUSIONS

This chapter has three sections. The first section gives all the hydraulic design parameters necessary to design ring chambers. The second section compares results from this study with those results obtained from studies on prototype ring chamber tests. The velocity reduction curve is calibrated based on these tests. The third section gives the procedure to design ring chambers.

Section 5.1 Hydraulic Design Parameters

Of the three sets of tests the two for fully choked flow allow for higher Froude numbers and inlet relative depths. There is not a large difference between the results for the two sets with fully choked flow (see Figures 4.1.7 to 4.1.9), so it is best to use the ring chamber design that would be less expensive to construct. Therefore the design with three 2-piece dissipators (see Figure 2.2.5), $K/D_0 = 1/6$ and $L/D_0 = 1.0$ should be chosen over the design with four 2-piece dissipators, $K/D_0 = 1/8$ and $L/D_0 = 1.0$ because it allows for a shorter ring chamber (usually, at least 20% shorter). Thus the design should follow data presented in Figure 4.1.6.

Figure 5.1.1 is a reproduction of Figure 4.1.6 with the D_0/D_i lines lengthened to show the range over which they are supported by experimental tests. All four lines stretch from relative inlet values of 0.60 to Froude numbers of 7.0.

This graph may be used as a design aid to determine choked flow conditions in ring chambers of various sizes. Designs with relative inlet depths and inlet Froude numbers falling on or below these lines are acceptable.

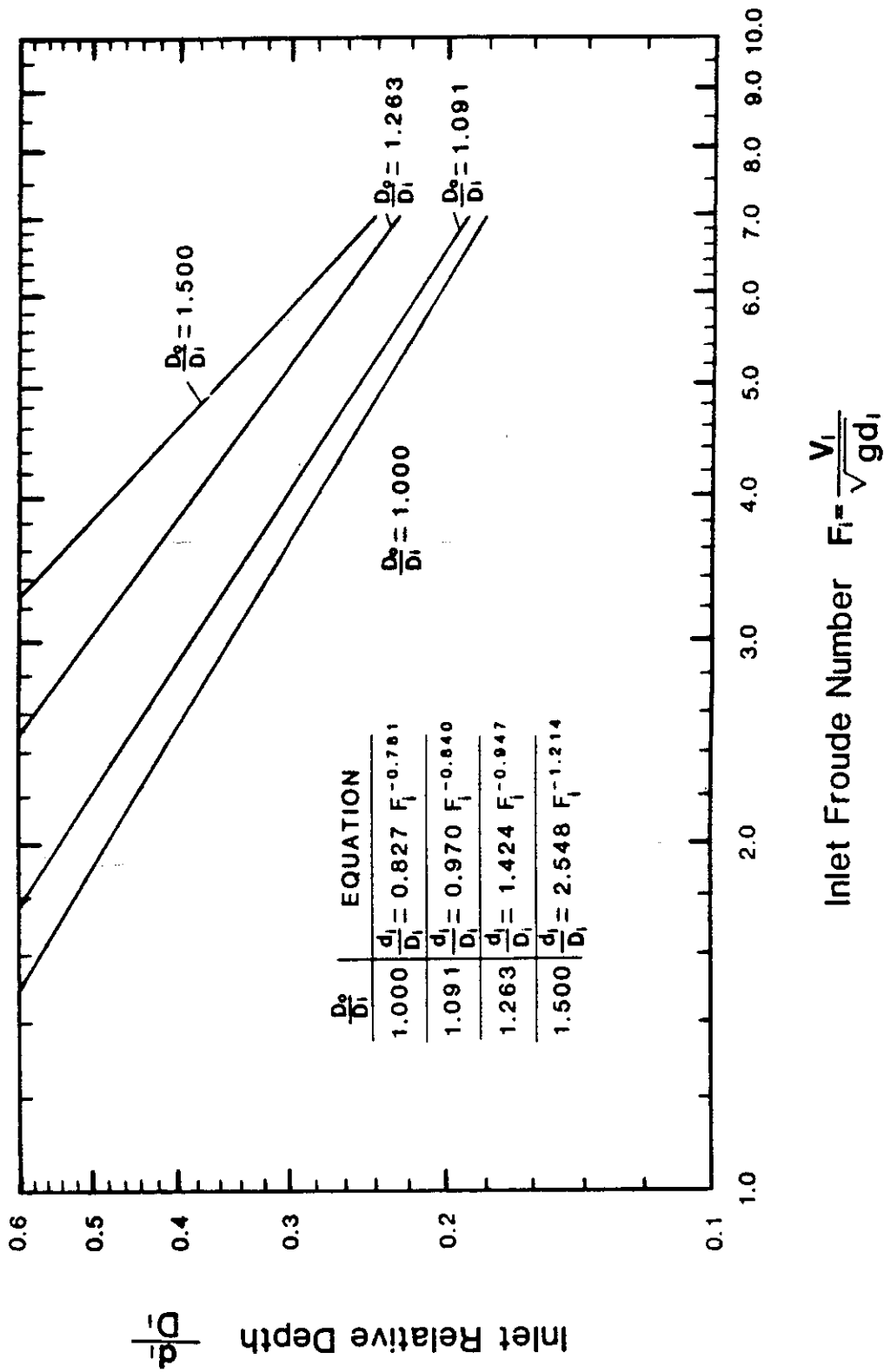


FIGURE 5.1.1 SUMMARY GRAPH FOR FULLY CHOKED CONDITIONS

Other hydraulic design parameters are discussed below.

Slope

All results in Tables 4.1.1.a - 4.1.1.c were obtained with the ring chamber on a 0.005 ft/ft slope. Slight variations from this slope did not affect the dissipative performance of the chamber. It is recommended that the slope be kept in the range of 0.002 ft/ft to 0.007 ft/ft.

Distance to First Dissipator

The distance from the beginning of the ring chamber to the first dissipator, L_1 , should be 1.33 diameter lengths long. If it is less than this value and the inlet pipe to ring chamber is built as in Figure 3.1.1, Section B-B, the flow could shoot over the first dissipator.

Drainage Gap

The drainage gap, G , between the two elements that make up each dissipator was sized by the Ohio Department of Transportation [14] to be in the range:

$$\frac{1}{13} < G/D_0 < \frac{1}{6.5} \quad (5.1.1)$$

In this study, $G/D_0 = 1/8$. Therefore, it is recommended that

$$\frac{1}{13} < G/D_0 < \frac{1}{8} \quad (5.1.2)$$

To make Table 5.3.1, G/D_0 was set equal to 1/8.

Dissipator Thickness

The dissipator heights, K , as listed in Table 5.3.1 are according to those given by the Ohio Department of Transportation [14] and are based on structural considerations.

Settling Distance

The settling distance, L_s , is the distance from the last dissipator to the end of the culvert. In this region water held back by the last dissipator quickly tumbles to a lesser depth and attains a greater velocity. The settling distance should be long enough so that the vertical velocity component downward does not increase the erosion potential at the culvert's exit. This acceleration to a lesser depth is completed within a two-diameter distance after the last dissipator.

Venting

When a hydraulic jump in the ring chamber is produced it can cause a negative pressure in the inlet pipe that works with the load above in trying to crush the inlet pipe. This negative pressure can be relieved by venting the pipe anywhere upstream of the hydraulic jump (see Figure 5.1.2). It is known that venting causes the exiting velocity to increase but the amount of increase is unknown because in the models venting causes the outlet velocity to be too turbulent to accurately measure. If venting is desired, the diameter of the ring chamber should be increased to the next available size than determined by the design procedure in Section 5.3 (other hydraulic parameters should increase for the new D_0 as in Table 5.3.1). This will decrease the exiting velocity and tend to compensate for the venting effects. In an unvented ring chamber the maximum possible pressure reduction is 14.7 psi. Assuming the unit weight of the soil cover to be 120 lbs/ft³, or 0.833 lbs per in² per foot of cover depth, the maximum pressure reduction in the pipe would be equivalent to an increase of 17.6 ft. in soil cover.

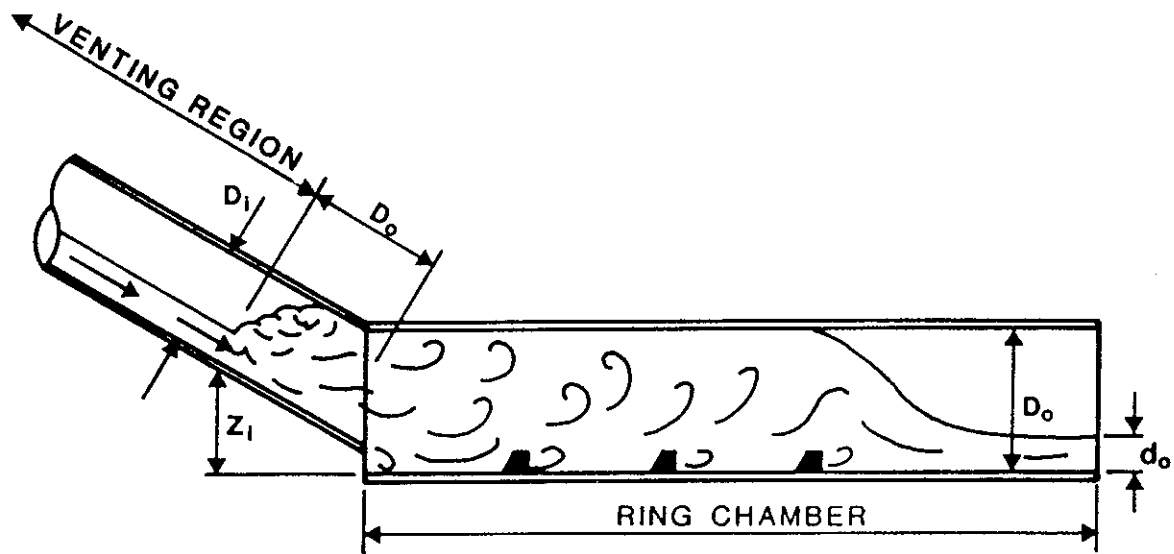


FIGURE 5.1.2 VENTING REGION

Tailwater Effects

The results in this report were obtained with no tailwater effects. Any tailwater associated with the prototype would tend to be conservative. A tailwater with a depth greater than $1.5d_0$ would reduce the outlet velocity a few percent more than that given by Equation 5.2.2 below.

Section 5.2 Prototype Ring Chamber Tests and Model Calibration

In reference [22] tests were done in models similar to those tested in this study. The results for 6-inch diameter models were compared to results obtained from tests on an 18-inch prototype concrete culvert under the same flow conditions. Similar tests were also reported by Sarikelle and Simon [18] in an 84 inch ring chamber with a 60 inch inlet pipe (in these tests the ring chamber only flowed 61-64% full). The results obtained from these studies are listed in Table 5.2.1.

TABLE 5.2.1 COMPARISON OF MODEL AND PROTOTYPE ENERGY REDUCTIONS

MODEL DIAMETER (D ₀ IN.)	PROTOTYPE DIAMETER (D ₀ IN.)	% MODEL ENERGY REDUCTION	% PROTOTYPE ENERGY REDUCTION	% DIFF. IN ENERGY REDUCTION
6	18	87.2	65.0	25.5
6	18	83.6	53.0	36.6
6	84	90.0*	55.8	38.0
6	84	90.0*	60.2	33.1

*Estimated value based on results in Reference [18].

The differences in energy reductions between the model and prototypes are because of viscous forces that are of lesser magnitude than gravity forces but still significant. As a pipe's diameter decreases, the percentage of the total energy losses due to viscous forces increase. Thus it would be expected that there would be more energy reduction in the model than in the prototype. Based on this and the results reported in the final column of Table 5.2.1 it is recommended that for prototype designs the energy and velocity reduction values obtained by Equations 4.2.1 and 4.3.1 be reduced 33.3 percent.

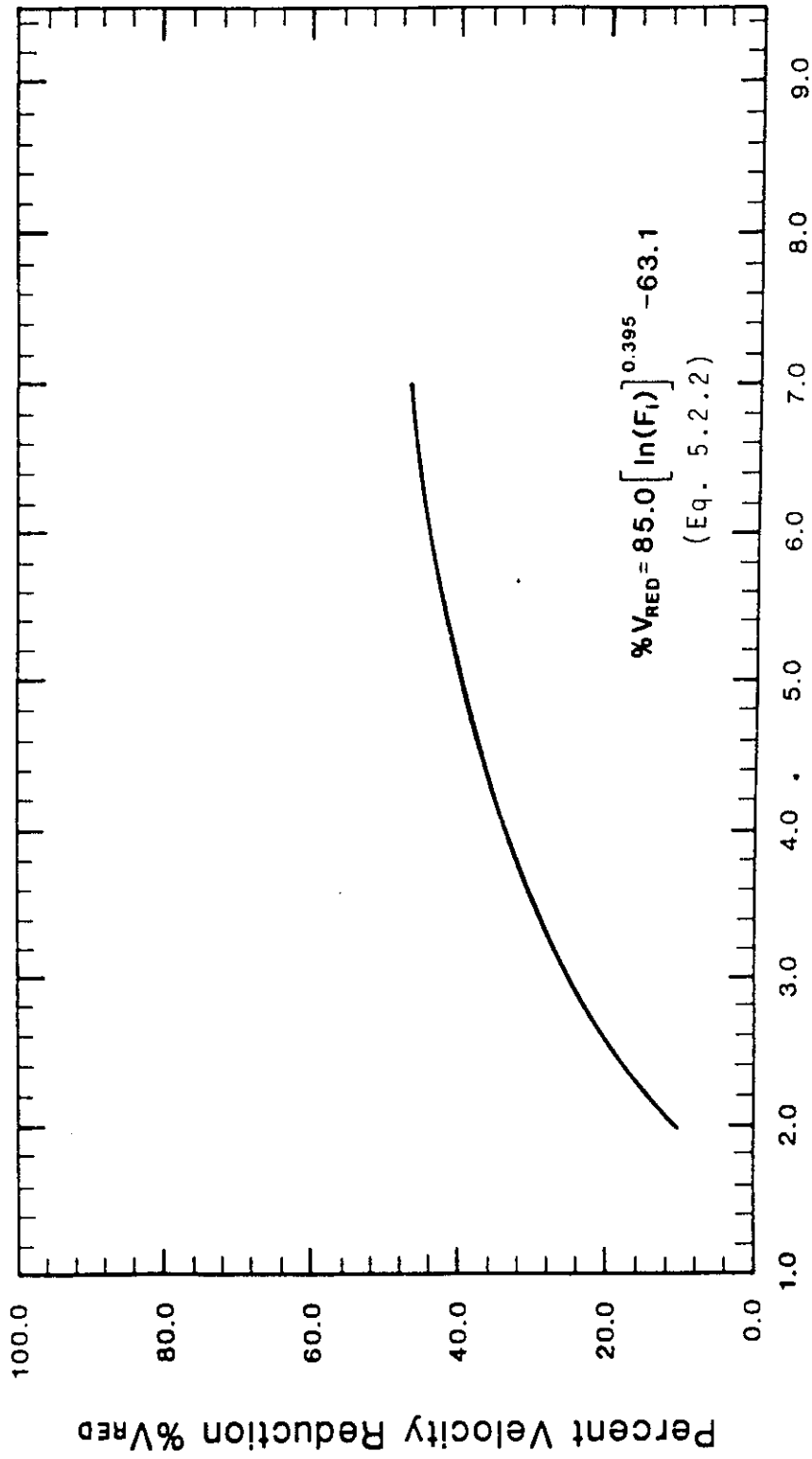
The calibrated energy reduction equation becomes

$$\% E_{RED} = 106.9 [\ln (F_i)]^{0.347} - 75.6 \dots \dots (5.2.1)$$

The calibrated velocity reduction equation becomes

$$\% V_{RED} = 85.0 [\ln (F_i)]^{0.395} - 63.1 \dots \dots (5.2.2)$$

Figure 5.2.1 is of Equation (5.2.2). This graph should only be used for culverts 18 in. or greater in diameter.



Inlet Froude Number $F_i = \frac{V_i}{\sqrt{g d_i}}$

FIGURE 5.2.1 CALIBRATED PERCENT VELOCITY REDUCTION CURVE

Section 5.3 Design Procedure

The steps necessary to design a ring chamber based on the results of this study are given below.

1. Find Outlet Velocity

Find the outlet velocity of the culvert without a ring chamber on it. This can be accomplished by using information given in References [6,7,8,17] or any other approved design manuals and/or procedures. If the computed outlet velocity is greater than 18 ft/sec and the culvert is flowing under inlet control, a ring chamber based on this study can be used to reduce the outlet velocity.

2. Assume Ring Chamber Diameter Size, D_o

Assume a ring chamber to inlet ratio, D_o/D_i . To start with choose that diameter of ring chamber from commercially available culvert sizes such that D_o/D_i is close to 1.25. The length of the ring chamber L_o is then obtained from Table 5.3.1.

3. Find New Slope of Inlet Pipe

Find the new slope of the inlet pipe now that a ring chamber with a slope of 0.002 ft/ft to 0.007 ft/ft is to be attached to it. This involves some simple trigonometry.

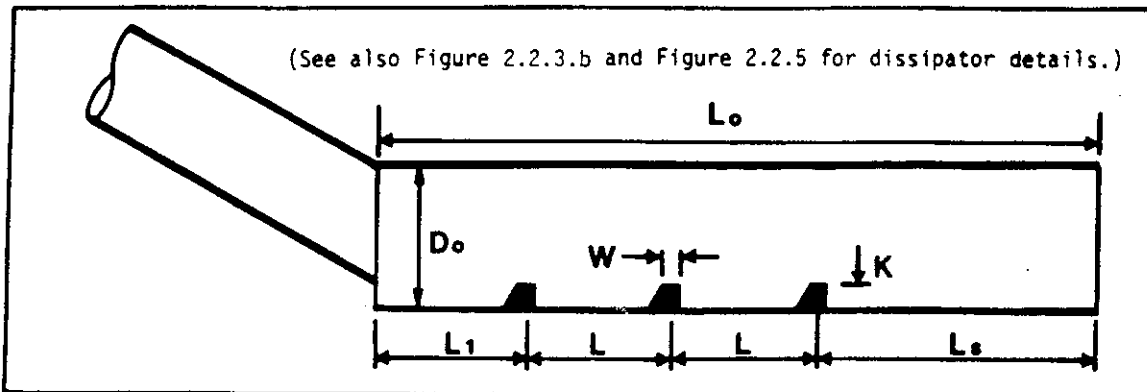
4. Find New Inlet Velocity and Normal Depth

Find the new velocity and normal depth at the end of the culvert just as in step 1 above but with the new slope found in step 3.

5. Check Figure 5.1.1

Find F_j and check Figure 5.1.1 to see if the assumed ring chamber size was correct. If not, repeat steps 2 to 4 with increasingly larger or smaller ring chamber diameters until the result checks with those

TABLE 5.3.1 RING CHAMBER DESIGN GUIDE



D_o (in.)	D_o (ft.)	L_1 (ft.)	L (ft.)	L_s (ft.)	L_o (ft.)	K (in.)	G (in.)	W (in.)
36	3	4	3	6	16	6	4	7
42	3-1/2	6	4-1/2	9	24	7	5	7
48	4	6	4-1/2	9	24	8	6	8
54	4-1/2	6	4-1/2	9	24	9	6	8
60	5	8	6	12	32	10	7	9
66	5-1/2	8	6	12	32	11	8	9
72	6	8	6	12	32	12	9	9
78	6-1/2	10	7-1/2	15	40	13	9	9
84	7	10	7-1/2	15	40	14	10	9
90	7-1/2	10	7-1/2	15	40	15	11	9
96	8	12	9	18	48	16	12	10
102	8-1/2	12	9	18	48	17	12	10
108	9	12	9	18	48	18	13	10
114	9-1/2	14	10-1/2	21	56	19	14	10
120	10	14	10-1/2	21	56	20	15	10
126	10-1/2	14	10-1/2	21	56	21	15	12
132	11	16	12	24	64	22	16	12
138	11-1/2	16	12	24	64	23	17	12
144	12	16	12	24	64	24	18	12
150	12-1/2	18	13-1/2	27	72	25	18	12
156	13	18	13-1/2	27	72	26	19	12
162	13-1/2	18	13-1/2	27	72	27	20	15
168	14	20	15	30	80	28	21	15
174	14-1/2	20	15	30	80	29	21	15
180	15	20	15	30	80	30	22	15

shown in Figure 5.1.1. (For D_o/D_i values not represented by equations on Figure 5.1.1 it is necessary to linearly interpolate between the two closest lines that are represented by equations. For instance, if $D_o/D_i = 1.4$ it is necessary to linearly interpolate between the lines $D_o/D_i = 1.263$ and $D_o/D_i = 1.500$.)

6. Find Reduced Outlet Velocity

Find the reduced outlet velocity with Equation 5.2.2 or Figure 5.2.1. If the outlet velocity is greater than 18 ft/sec additional measures will be needed to reduce this velocity.

7. Check if Venting is Necessary

If venting is necessary, the diameter of the ring chamber should be increased to the next available size greater than that found in step 5 above. Whether or not venting is necessary, find other hydraulic parameters for the design D_o value from Table 5.3.1.

REFERENCES

1. Bakhmeteff, B.A., and Matzke, A.E., "The Hydraulic Jump in Terms of Dynamic Similarity," Transactions, ASCE, Vol. 101, 1936, pp. 630-647.
2. Bevington, P.R., Data Reduction and Error Analysis for the Physical Sciences, McGraw-Hill Book Co., New York, N.Y., 1969.
3. Bradley, J.N., and Peterka, A.J., "The Hydraulic Design of Stilling Basins: Hydraulic Jumps on a Horizontal Apron (Basin I)," Journal of the Hydraulics Division, ASCE Vol. 83, No. H15, Proc. Paper 1401, Oct., 1957, pp. 1401-1 to 1401-24.
4. Bradley, J.N., and Peterka, A.J., "Hydraulic Design of Stilling Basins for Canal Structures, Small Outlet Works, and Small Spillways (Basin III)," Journal of the Hydraulics Division, ASCE Vol. 83, No. H15, Proc. Paper 1403, Oct., 1957, pp. 1403 to 1403-22.
5. Chow, V.T., Open-Channel Hydraulics, McGraw-Hill Book Co., New York, N.Y., 1959.
6. Federal Highway Administration, Design Charts for Open-Channel Flow, U.S. Department of Transportation, Washington, D.C., HDS No. 3, Mar. 1979.
7. Federal Highway Administration, Hydraulic Charts for the Selection of Highway Culverts", U.S. Department of Transportation, Washington, D.C., HEC No. 5, Dec., 1965.
8. Federal Highway Administration, Hydraulic Design of Energy Dissipators for Culverts and Channels, U.S. Department of Transportation, Washington, D.C., HEC No. 14, Nov., 1975.
9. Federal Highway Administration, Hydraulic Design of Improved Inlets for Culverts, U.S. Department of Transportation, Washington, D.C., HEC No. 13, Aug., 1972.
10. Henderson, F.M., Open Channel Flow, MacMillan Publishing Co., Inc., New York, N.Y., 1966.
11. "Hydraulic Models", Manual of Engineering Practice No. 25, Committee of the Hydraulics Division on Hydraulic Research, ASCE, 1942.
12. Korom, S.F., "Optimum Design of Internal Energy Dissipators for Culverts Operating Under Inlet Control", thesis presented to the University of Akron in 1984 in partial fulfillment for the degree of Master of Science.
13. Morris, H.M., and Wiggert, J.M., Applied Hydraulics in Engineering Ronald Press Co., New York, N.Y., 1972.

14. Pettit, C.G., "Internal Energy Dissipation for the High Energy Conduit", Ohio Department of Transportation, Columbus, Ohio, Unpublished.
15. Pettit, C.G., "Ring Chambers for High Energy Conduits", Ohio Department of Transportation, Columbus, Ohio, Jan. 1980. Unpublished.
16. Pettit, C.G., "The Enclosure of Permars Run", Concrete Pipe News, Feb., 1980, pp. 7-11.
17. Portland Cement Association, Handbook of Concrete Culvert Pipe Hydraulics, Skokie, Illinois, 1964.
18. Sarikelle, S., and Simon, A.L., "Field and Laboratory Evaluation of Energy Dissipators for Culvert and Storm Drain Outlets", Vol. 1, University of Akron, Akron, Ohio, Dec., 1980.
19. Silvester, R., "Hydraulic Jump in All Shapes of Horizontal Channels", Journal of the Hydraulics Division, ASCE, Vol. 90, No. HY1, Proc. Paper 3754, Jan., 1964, pp. 23-55.
20. Simon, A.L., Practical Hydraulics, Second Edition, John Wiley & Sons, New York, N.Y., 1981.
21. Wiggert, J.M., and Eifle, P.D., "Culvert Velocity Reduction by Internal Energy Dissipators," Concrete Pipe News, Oct., 1972, pp. 87-93.
22. Wiggert, J.M., Eifle, P.D., and Morris, H.M., "Roughness Elements as Energy Dissipators of Free-Surface Flow in Circular Pipes," Highway Research Record, Record No. 373, 1972, pp. 64-73.

APPENDIX - SAMPLE PROBLEM

A culvert needs to transport 130 cfs of water through a horizontal distance of 300' and a vertical distance of 24'. Tailwater is 3.0'. Hydraulic analysis indicates the culvert would be under inlet control and 48" in diameter. Is a ring chamber necessary, if so, what is its design?

1. Find Outlet Velocity.

$$Q = 130 \text{ cfs} \quad \text{Assume } n = 0.012$$

$$\text{slope} = 24/300 = 0.08 \text{ ft/ft}$$

$$\text{From Reference [6]} \quad \text{Depth} = 1.45 \text{ ft.}$$

$$V_i = 30 \text{ ft/s}$$

30 ft/sec > 18 ft/sec so a ring chamber is needed.

2. Assume Ring Chamber Diameter Size, D_o

$$\text{Assume } D_o = 60'' \quad \frac{D_o}{D_i} = \frac{60}{48} = 1.25$$

$$\text{From Table 5.3.1} \quad L_{o60''} = 32 \text{ ft.}$$

3. Find New Slope of Inlet Pipe

$$\text{Slope of ring chamber} = 0.005 \text{ ft/ft}$$

$$\text{Elevation} = 0.005(32) = 0.16'$$

$$\text{Remainder} = 24 - 0.16 = 23.84'$$

$$\begin{aligned} \text{Slope of inlet pipe} &= \frac{23.84}{276} \\ &= 0.086 \text{ ft/ft} \end{aligned}$$

4. Find New Inlet Velocity and Normal Depth

From Reference [6] Depth = 1.43 ft.

$$V_i = 31 \text{ ft/s}$$

5. Check Figure 5.1.1

$$F_i = \frac{31}{[g(1.43)]^{1/2}} = 4.6$$

Allowable $\frac{d_i}{D_i} = 1.424(4.6)^{-0.947} = 0.34$ for $\frac{D_o}{D_i} = 1.263$, appr. 1.25

Actual $\frac{d_i}{D_i} = \frac{1.42}{4} = 0.36 > 0.34$ N.G. Repeat steps 2-4 with $D_o=66''$

2. Assume New Ring Chamber Diameter Size, D_o

$$\text{New } D_o = 66''$$

$$\frac{D_o}{D_i} = \frac{66}{48} = 1.375$$

From Table 5.3.1 $L_{066''} = 32 \text{ ft.}$

3. Find New Slope of Inlet Pipe.

Since $L_{066''} = 32 \text{ ft.}$, slope of inlet size remains equal to 0.086 ft/ft.

4. Find New Inlet Velocity and Normal Depth.

From step 4 above Depth = 1.43 ft

$$V_i = 31 \text{ ft/s}$$

$$V_0 = 19.4 \text{ ft/sec} > 18.0 \text{ ft/s} \quad \text{Check tailwater}$$

$$A_0 = \frac{130 \text{ cfs}}{19.4 \text{ ft/s}} = 6.70 \text{ ft}^2$$

$$\text{From standard circular section tables, } \frac{A_0}{D_0^2} = \frac{6.70}{(5.5)^2} = 0.221,$$

$$\text{yields } \frac{d_0}{D_0} = 0.324. \quad d_0 = 1.78 \text{ ft.}$$

$$1.5d_0 = 2.67 \text{ ft} < 3.0 \text{ ft} \quad \text{Tailwater controls.}$$

Since the tailwater $> 1.5d_0$, it can be assumed that V_0 can be further reduced a few percent which would make V_0 approximately equal to 18 ft/s.

7. Check if venting is necessary.

If a vent is added D_0 should be increased to the next size or 72".

Find hydraulic parameters from Table 5.3.1.

If a vent is added:

$$D_0 = 72''$$

$$L_1 = 8'$$

$$L = 6'$$

$$L_S = 12'$$

$$L_0 = 32'$$

$$K = 12''$$

$$G = 9''$$

$$W = 9''$$

If a vent is not added:

$$D_0 = 66''$$

$$L_1 = 8'$$

$$L = 6'$$

$$L_S = 12'$$

$$L_0 = 32'$$

$$K = 11''$$

$$G = 8''$$

$$W = 9''$$